Diploma Thesis

Echocardiographic parameters as predictors of cardiac decompensation after transjugular intrahepatic portosystemic shunt

submitted by

Anna Neuhuber

for the Academic Degree of

Doktor(in) der gesamten Heilkunde

(Dr^{in}. med. univ.)

at the

Medical University of Graz

executed at the

University departments of Internal Medicine

executed at the

Division of Cardiology

under the Supervision of

Dr.med.univ. Nora Schwegel

Dr.scient.med. Dr.med.univ. Ewald Kolesnik

Priv.-Doc. Dr.scient.med Dr.med.univ. Dirk von Lewinski

Graz, 18.09.2025

Statutory Declaration

I hereby declare, on my word of honour, that I have written this thesis independently and without unauthorized assistance. I have not used any sources or resources other than those explicitly stated. All passages that are taken directly or indirectly from published or unpublished sources are clearly marked and achknowledged as such.

Furthermore, I hereby declare that if artificial intelligence (AI) tools were used to generate and/or correct certain text passages in the creation of this work, this use was carried out in compliance with ethical principles, academic integrity and the requirements of my university, and subsequently made transparent and appropriately identified.

Graz, 18.09.2025 Anna Neuhuber, m.p.

Acknowledgement

I am sincerely grateful to both my supervisors, Dr.med.univ. Nora Schwegel and Dr.scient.med.Dr.med.univ.Ewald Kolesnik, for their invaluable guidance and assistance throughout my studies and writing process. I truly appreciated their availability at all hours, thoughtful advices, and steady support every step of the way.

A very special thank you goes as well to my family and friends for their limitless support throughout this journey.

Abstract

Background and Aim: The implantation of a transjugular intrahepatic portosystemic shunt (TIPS) is a therapeutic option for patients with advanced liver disease. However, approximately 20% of patients develop acute heart failure within one year after the procedure. The main cause of death in patients with cirrhosis who have undergone a TIPS procedure is cardiac decompensation. The mechanisms are most likely either the presence of cirrhotic cardiomyopathy and/or volume changes after the TIPS implantation.

Additionally, the study seeks to evaluate the efficacy of the Toulouse algorithm as a decision-making tool for risk assessment prior to the TIPS procedure.

Material and Methods: This is a retrospective analysis of a prospective registry conducted at the Department of Hepatology, Medical University of Graz. All patients with echocardiographic studies performed six months prior to or following the TIPS procedure were enrolled in the present study.

Results: A total of 74 patients with a median (interquartile range) age of 60 years (53-67) including 27 females (37%) were enrolled between 01.02.-01.07.2025. The median mean arterial pressure (MAP) was 81mmHg (74-91), the median body mass index (BMI) was 24.8 kg/m² [21.7-29.4], and 23 patients had diabetes mellitus (31%). Alcohol-related liver cirrhosis was the most common etiology (n=55), with refractory ascites as the primary indication for TIPS (n=36), followed by recurrent (n=14) and active (n=14) gastrointestinal bleeding. Based on echocardiographic parameters from the Toulouse algorithm, comprising E/A, E/e', and left atrial volume index (LAVI), patients were stratified to a low risk (n=24) and high risk group (n=32). Parameters depicting systolic function of the left and right ventricle did not differ between groups. However, patients in the low risk group had significantly less tricuspid regurgitation (maximal velocity 14 vs 26 cm/s, p = <0,001).

Conclusion: Our findings demonstrate that echocardiographic parameters play a vital role in the risk assessment of patients undergoing transjugular intrahepatic portosystemic shunt (TIPS) placement. The data suggest the presence of preexisting cardiac dysfunction, particularly in high-risk patients, and emphasize the prognostic significance of diastolic function parameters, especially the TRVmax, prior to TIPS implantation. As a result, we

strongly recommend that a structured cardiologic evaluation be established as an integral component of the preoperative assessment process. Such an approach would facilitate the early identification of cardiac comorbidities, allowing clinicians to recognize patients at increased risk and take appropriate preventive measures. This could help reduce the likelihood of cardiac decompensations following theTIPS procedure and contribute to improved overall patient management.

Zusammenfassung

Hintergrund und Ziel: Die Implantation eines transjugulären intrahepatischen portosystemischen Shunts (TIPS) stellt eine therapeutische Option für Patienten und Patientinnen mit fortgeschrittener Lebererkrankung dar. Allerdings entwickeln etwa 20 % der Patienten und Patientinnen innerhalb eines Jahres nach dem Eingriff eine akute Herzinsuffizienz. Die Haupttodesursache von Patienten und Patientinnen mit Zirrhose, die sich einer TIPS-Operation unterzogen haben, ist die kardiale Dekompensation. Die zugrundeliegenden Mechanismen sind höchstwahrscheinlich das Vorhandensein einer zirrhotischen Kardiomyopathie und/oder die Volumenveränderungen nach der TIPS-Implantation.

Darüber hinaus soll die Studie die Wirksamkeit des Toulouse-Algorithmus als Entscheidungsinstrument für die Risikobewertung vor dem TIPS-Eingriff evaluieren.

Material und Methoden: Dies ist eine retrospektive Analyse eines prospektiven Registers, welches an der Abteilung für Hepatologie der Medizinischen Universität Graz durchgeführt wurde. Alle Patienten und Patientinnen mir verwertbaren tranksthorakalen Echokardiogrammen sechs Monate vor oder nach der TIPSImplantation, wurden in die vorliegende Studie eingeschlossen.

Resultate: Insgesamt wurden 74 Patienten und Patientinnen zwischen 01.01. und 01.07.2025 mit einem medianen (Interquartilsbereich) Alter von 60 Jahren (53-67), darunter 27 Frauen (37%), eingeschlossen. Der mediane durchschnittliche arterielle Blutdruck (MAP) betrug 81 mmHg (74-91), der mediane Body-Mass-Index (BMI) lag bei 24,8 kg/m² (21,7-29,4), und 23 Patienten und Patientinnen (31%) litten an Diabetes Mellitus. Die alkoholbedingte Leberzirrhose war mit 75% die häufigste
Ätiologie (n=55). Die Hauptindikation für die TIPS-Implantation stellten refraktärer Aszites (n=36), gefolgt von rezidivierenden (n=14) und aktiven (n=14) gastrointestinalen Blutungen dar. Basierend auf echokardiografischen Parametern des Toulouse-Algorithmus, der E/A, E/e' und den linken Vorhofvolumenindex (LAVI) umfasst, wurden die Patienten und Patientinnen in eine niedrige Risikogruppe (n=24) und eine hohe Risikogruppe (n=32) eingeteilt. Parameter, die die systolische Funktion des linken und rechten Ventrikels

beschreiben, wiesen keine signifikanten Unterschiede zwischen den Gruppen auf. Patienten und Patientinnen in der niedrigen Risikogruppe zeigten jedoch eine geringer augeprägte Trikuspidalinsuffizienz (maximale Geschwindigkeit 14 vs. 26 cm/s, p = <0,001).

Fazit: Unsere Ergebnisse zeigen, dass echokardiografische Parameter eine wesentliche Rolle in der präinterventionellen Risikoeinschätzung vor TIPS spielen. Unsere Daten deuten auf eine bereits präexistente kardiale Belastung hin und unterstreichen die prognostische Relevanz vor allem von diastolischer Funktionsparameter, im Speziellen von der TRVmax, im Vorfeld einer TIPSImplantation. Eine strukturierte kardiologische Abklärung sollte daher integraler Bestandteil des präoperativen Assessments sein, um kardiale Vorbelastungen frühzeitig zu erkennen und das postinterventionelle Risiko zu minimieren.

Table of Contents

Abbreviations and Definitions

%	Percentages
2D	Two-Dimensional
3D	Three-Dimensional
A2C	Apical Two Chamber View
A3C	Apical Three Chamber View
A4C	Apical Four Chamber View
AC	Alcoholic Cardiomyopathy
ACE	Angiotensin-Converting Enzyme
ALD	Alcohol-Associated Liver Disease
Ao	Aorta
BNP	Brain Natriuretic Peptide
BSA	Body Surface Area
B-mode	Brightness Mode
CCM	Cirrhotic Cardiomyopathy
CHE	Congestive Heart Failure
cm	Centimeter
cm^2	Square Centimeters
cm^3	Cubic Centimeters
CO	Carbon Monoxide
CW	Continuous Wave
DCM	Dilated Cardiomyopathy
DT	Deceleration Time
E/A	Ratio Of Early To Late Left Ventricular Filling Velocity
E/e‘	Ratio Of Early Diastolic Transmitral Flow To Early Diastolic Mitral Annular Tissue Velocity
EF	Ejection Fraction
ELGA	Elektronische Gesundheitsakte
ESC	European Society Of Cardiology
e‘ (E Prime)	Early Diastolic Mitral Annular Velocity
GLS	Global Longitudinal Strain
HCC	Hepatocellular Carcinoma
HCM	Hypertrophic Cardiomyopathy
HFpEF	Heart Failure With Preserved Ejection Fraction
HFrEF	Heart Failure With Reduced Ejection Fraction
iDCM	Idiopathic Dilated Cardiomyopathy
IVRT	Isovolumetric Relaxation Time
IVSed	Interventricular Septum
LA	Left Atrium
LA_diameter	Left Atrial Diameter
LAarea_ES	End-Systolic Left Atrial Volume
LAlength_ES	End-Systolic Maximal Lengths Of Left Atrium

LAV_ES	End-Systolic Left Atrial Volume
LAVI	Left Atrial Volume Index
LV	Left Ventricle
LVEDD	Left Ventricular End-Diastolic Diameter
LVEDV	Left Ventricular End-Diastolic Volume
LVEF	Left Ventricular Ejection Fraction
LVESV	Left Ventricular End-Systolic Volume
LVGLS	Left Ventricular Global Longitudinal Strain
MAP	Median Arterial Pressure
MASH	Metabolic Dysfunction–Associated Steatohepatitis
mm	Millimeters
M-mode	Motion Mode
MV	Mitral Valve
m/s	Meters Per Second
NASH	Nonalcoholic Steatohepatitis
NO	Nitric Oxide
Nt-pro-BNP	N-Terminal Pro-B-Type Natriuretic Peptide
PPH	Porto-Pulmonary Hypertension
PLAX	Parasternal Long-Axis View
PWed	Posterior Wall Thickness
PW	Pulsed Wave
QTc	Corrected QT Interval
RA	Right Atrium
RAarea_ES	End-Systolic Right Atrial Volume
RAlength_ES	End-Systolic Maximal Lengths Of Right Atrium
RAV_ES	End-Systolic Right Atrial Volume
RAAS	Renin-Angiotensin-Aldosterone System
RAVI	Right Atrial Volume Index
ROS	Reactive Oxygen Species
RV	Right Ventricle
RV4CSL	Right Ventricular Four-Chamber Longitudinal Strain
RVAd	End-Diastolic Right Ventricular Volume
RVAs	End-Systolic Right Ventricular Volume
RVEDD_basal	End-Diastolic Right Ventricular Basal Diameter
RVEDD_mid	End-Diastolic Right Ventricular Mid Diameter
RVEDL	End-Diastolic Right Ventricular Maximal Length
RVFAC	Right Ventricle Fractional Area Change
RVFWSL	Right Ventricular Free Wall Longitudinal Strain
s‘ (S Prime)	Systolic Mitral Annular Velocity
SNS	Sympathetic Nervous System
TAPSE	Tricuspid Annular Plane Systolic Excursion
TDI	Tissue Doppler Imaging

TEE	Transesophageal Echocardiography
TIPS	Transjugular Intrahepatic Portosystemic Shunt
TR	Tricuspid Regurgitation
TRV	Tricuspid Regurgitation Peak Velocity
TRVmax	Tricuspid Regurgitant Velocity Maximum
TTE	Transthoracic Echocardiography
TV	Tricuspid Valve
VCI	Vena Cava Inferior

List of Figures

List of Tables

1 Introduction

1.1 Livercirrhosis: Epidemiology and Prevalence

Europe has the largest burden of liver diseases in the world, an expected growth across many countries in Europe as well as globally.[1], [2]

In Central Europe liver diseases are the leading cause of death among young adults aged 25-44, with alcohol-associated liver disease (ALD) being the most common cause. As obesity rates continue to increase, metabolic dysfunction-associated steatotic liver disease (MASLD) rises faster than ever. Furthermore, our region has the highest global prevalence of both compensated and decompensated cirrhosis. [3]

Liver cirrhosis worldwide lead to 1.48 million deaths in 2019, what shows a growth of 8.1% compared to 2017. [1]

The highest letality due to liver cirrhosis in Europe was shown in south-eastern and north-eastern Europe. [4]

The analysis of mortality rates from 1959 to 2002 revealed a significant East-to-West gradient in liver cirrhosis mortality across Europe. The burden of liver cirrhosis deaths increased notably in two regions of Eastern Europe: South-eastern and North-eastern Europe. In South-eastern Europe, liver cirrhosis mortality rates were 10 to 20 times higher than in most other European countries. In North-eastern Europe, including the former Soviet Union countries, liver cirrhosis mortality showed dramatic fluctuations, with periods of both increase and decrease. While liver cirrhosis has multiple contributing factors, alcohol consumption appears to be the primary driver of the observed patterns in mortality rates across Europe. The implementation of stricter alcohol control policies in Central and Eastern Europe could significantly reduce premature deaths from liver cirrhosis.[5]

1.1.1 Liver Cirrhosis: Pathophysiology

Liver cirrhosis occurs as the final stage of chronic liver disease. Its clinical progression is influenced by the underlying cause and associated risk factors, which vary based on geographic and cultural contexts.[6]

In high-income countries, the majority of cirrhosis cases are caused by chronic alcohol consumption, chronic viral hepatitis (hepatitis B and C), or metabolic dysfunction–associated steatohepatitis (MASH, formerly known as nonalcoholic steatohepatitis/NASH). In certain regions of Asia and Africa, cirrhosis is mostly a result of chronic hepatitis B, which is endemic. Additionally, damage to the bile ducts can lead to cirrhosis, as seen in conditions like mechanical bile duct obstruction, primary biliary cholangitis, and primary sclerosing cholangitis.[7]

Initially, the liver injury leads to the formation of liver fibrosis, which is still reversible at this stage. However, if the damage persists, fibrosis progresses to cirrhosis, which is characterized by irreversible changes in the liver's structure and function.[8]

1.1.2 Transjugular intrahepatic portosystemic shunt (TIPS)

The main clinical outcomes of cirrhosis include redueced liver function, increased intrahepatic pressure with portal hypertension, esophageal varices and the potential development of hepatocellular carcinoma. Hepatic vascular changes und portal hypertension lead to circulatory changes, such as splanchnic vasodilation, vasoconstriction, kidney hypoperfusion, salt and water retention, and increased cardiac output.[9]

The transjugular intrahepatic portosystemic shunt (TIPS) is an intervention which effectively reduces the portal pressure in patients suffering from severe liver diseases.[10]

Portal hypertension is a central underlying mechanism of hepatic decompensation, leading to severe complications and low survival rates in patients with advanced liver cirrhosis, often with a median life expectancy of approximately two years, according to a systematic review of 118 studies from 2005 from the European Association for the Study of the Liver.[11], [12]

Due to the high pressure in the splanchic system, consequences such as refractory ascites and severe esophageal variceal bleedings may accure. The creation of a TIPS has become a standard approach for treating these portal hypertensionrelated complications in carefully selected patients.[13]

In fact, the TIPS intervention currently represents the only effective and prompt approach to reduce portal venous pressure. The shunt itself is formed by placing a stent between the portal vein and the hepatic vein. This technique decreases portal resistance, enhances portal venous inflow, and immediately relieves mesenteric venous congestion, leading to a reduction in portal pressure by approximately 50 percent.[14]

The main indications for TIPS are recurrend or active variceal bleeding or refractory ascites. Additionally, TIPS is used for managing refractory hepatic hydrothorax, Budd-Chiari syndrome as well as the hepatorenal and hepato-pulmonary syndrome.[15]

1.1.1.2 Cardiac decompensation following TIPS

Despite careful patient selection for TIPS treatment, two major complications still limit its use: hepatic encephalopathy and cardiac decompensation.[13]

Studies have shown that cardiac decompensation is the leading cause of death in patients with cirrhosis after a TIPS. Approximately 20% of patients develop acute heart failure within one year after the TIPS implantation.[15]

The creation of a portosystemic shunt induces abrupt hemodynamic changes, including reduced intrahepatic resistance and increased cardiac preload, which in turn raise ventricular filling pressure. If the heart fails to adapt to these hemodynamic shifts, signs of heart failure may emerge, potentially uncovering an underlying cirrhotic or alcoholic cardiomyopathy that was previously undiagnosed.[13]

Cardiac decompensation increases mortality but also greatly diminishes quality of life, underscoring its critical importance of cardiac assessment prior to a TIPS procedure.[15]

However, risk factors for cardiac decompensation, specific echocardiographic parameters and their respective cut-offs remain poorly defined.[11]

1.2. Cirrhotic cardiomyopathy (CCM)

Chronic liver disease can ultimately progress to liver cirrhosis, with the disease's course primarily driven by its complications. The key mechanism behind these

complications in cirrhotic patients is portal hypertension. It leads to intestinal venous congestion and furthermore to the transfer of bacteria and endotoxins into the systemic circulation, triggering a subclinical inflammatory response. Regarding these mechanisms, the inflammatory state along with the diminished hepatic function and the impaired syntethesis of various metabolites, are linked to cardiac dysfunction in cirrhotic patients. Those with end-stage liver disease carry a five fold increased risk of developing heart failure, particularly heart failure with preserved ejection fraction (HFpEF). A frequently observed condition in patients with advanced liver disease is cirrhotic cardiomyopathy (CCM). It is defined as subclinical cardiac impairment characterized by reduced contractility especially during exercise and impaired diastolic relaxation with electrophysiological abnormalities, in patients with no prior heart condition.[15], [16], [17]

1.2.1 Pathophysiology of Cirrhotic Cardiomyopathy

Disrupted synthesis and metabolism of various substances lead to an imbalance between vasoconstrictive and vasodilatory mediators (mainly nitric oxide [NO] and carbon monoxide [CO]), resulting in a vasodilatory state, particularly in the splanchnic circulation. The reduction in the effective circulating blood volume triggers maximal activation of neurohumoral circulatory regulation mechanisms (sympathetic nervous system [SNS], renin-angiotensin-aldosterone system [RAAS], vasopressin, etc.), which in turn results in elevated cardiac output and a hyperdynamic circulatory state. Since the heart is already performing at a high capacity during rest, no adequate increase in stroke volume or contractility can be accomplished on demand, leading to systolic dysfunction.[15], [18]

Venous congestion in the intestines causes the translocation of bacteria and endotoxins into the systemic circulation. This results in a subclinical inflammatory state, which can damage myocytes and potentially lead to diffuse myocardial fibrosis, ultimately resulting in diastolic dysfunction.[15], [19]

The most frequently documented electrophysiological alterations in patients with CCM include prolongation of the heart rate corrected QT interval (QTc), chronotropic incompetence, and disruption between electrical and mechanical activity. QTcprolongation is estimated in up to 50% of patients with liver cirrhosis,

irrespective of the underlying issue of the cirrhosis. Additionally, QTc is associated with the severity of cirrhosis and is expected to normalize in 50% of cases following transplantation. The origin of electrophysiological changes in CCM is considered to be multifactorial, involving dislocation of cardioactive elements into the systemic circulation, ion channel modification, and autonomic malfunction.[15], [20], [21]

1.2.2 Diagnosis of Cirrhotic Cardiomyopathy

CCM is challenging to differentiate and diagnose. In most cases, no clinical signs of the disease are present at rest. Moreover, in severe liver cirrhosis, the signs of excess fluid throughout the body may conceal coexisting heart failure. The distinct pathophysiology of CCM requires a thorough approach for diagnosis, considering several findings such as clinical, echocardiographic, and biomarker data. When clinical decompensation occurs, patients commonly exhibiting signs of heart failure. It becomes especially significant when a stressor, such as fluid overload or a TIPS, disrupts the hemodynamics.[15], [22], [23]

The diagnostic criterias for CCM were first introduced at the Worl Congress of Gastroenterology in Montreal 2005 by the World Gastroenterology Organisation. These criteria were divided into three main categories. The first two categories focused on assessing systolic and diastolic function, while the third category included additional criteria, such as electrophysiological or structural cardiac alterations and laboratory results, including elevated levels of brain natriuretic peptide or N-terminal pro brain type natriuretic peptide (NT-proBNP). Given the remarkable progress in transthoracic echocardiography (TTE) over the last few years, new echocardiographic parameters have emerged for assessing systolic and diastolic function. Systolic dysfunction is commonly defined as a left ventricular ejection fraction (LVEF) below 50% or an average global longitudinal strain (GLS) below 18%. Diastolic dysfunction was defined with 3 out of 4 positive criterias as follows: septal e' <7cm/s, E/e' ratio >15, left atrial volume index (LAVI) >34 mL/m² and tricuspid regurgitation peak velocity (TRVmax) > 2.8m/s. These echocardiographic parameters will be explained in the following sections. An overview of the diagnostic criteria for CCM are displayed in Table 1.[15], [24], [25]

2005 Criteria	2020 Criteria
Systolic dysfunction (any of the following)	
LVEF <55% Blunted response to stress	LVEF ≤50% GLS with absolute value <18%
Diastolic dysfunction (any of the following)	Diastolic dysfunction (≥3 of the following)
E/A <1 DT >200 msec IVRT >80 msec	Septal e velocity <7 cm/sec E/e' ≥15 LAVI >34 mL/m² TR peak velocity >2.8 m/sec

LVEF, left ventricular ejection fraction; GLS, global longitudinal strain; E/A, ratio of early to late left ventricular filling velocity; DT, deceleration time; IVRT, isovolumetric relaxation time; E/e', ratio of early diastolic transmitral flow to early diastolic mitral annular tissue velocity; LAVI, left atrial volume index; TR, tricuspid regurgitation

Table 1: Diagnostic criteria for cirrhotic cardiomyopathy. World Congress of Gastroenterology

1.3 Alcoholic Cardiomyopathy (AC)

Besides CCM, which is mainly a consequence of an established liver cirrhosis, alcohol itself not only affects the liver but the heart as well. Heart disease related to excessive alcohol consumption is called alcoholic cardiomyopathy (AC). It is clinically defined with a dilated cardiomyopathy (DCM) phenotype. Both clinically and histologically, alcoholic cardiomyopathy cannot be distinguished from idiopathic dilated cardiomyopathy, making it a diagnosis of exclusion.[26], [27], [28]

The amount of alcohol typically required to cause AC is considered to be over 80 g/day over 5 years, although there is still some debate surrounding this definition.[29]

1.3.1 Pathophysiology of Alcoholic Cardiomyopathy

Alcohol can lead to excessive free radical formation and oxidative stress through at least three mechanisms: directly through the metabolism of ethanol to acetaldehyde and ethyl esters, its effects on antioxidant proteins and enzymes, and indirectly through the activation or alteration of neurohormonal systems such as the

sympathetic nervous system and the RAAS. Alcohol also disturbs the calcium homeostasis which leads to mitochondrial dysfunction and changes in the structure of contractile proteins.[26]

This results in apoptosis and necrosis of cardiomyocytes, and although the regeneration rate after cell death is low, mechanisms such as hypertrophy of the remaining cells, may initially compensate for the effects of myocyte death. However, reduced levels of myofibrillar proteins, combined with the expression of various isoforms of myosin, lead to decreased contractility. This ultimately results in left ventricular dilation and systolic dysfunction. AC in general is estimated to account for up to 50% of all unexplained dilated cardiomyopathies.[26], [30], [31]

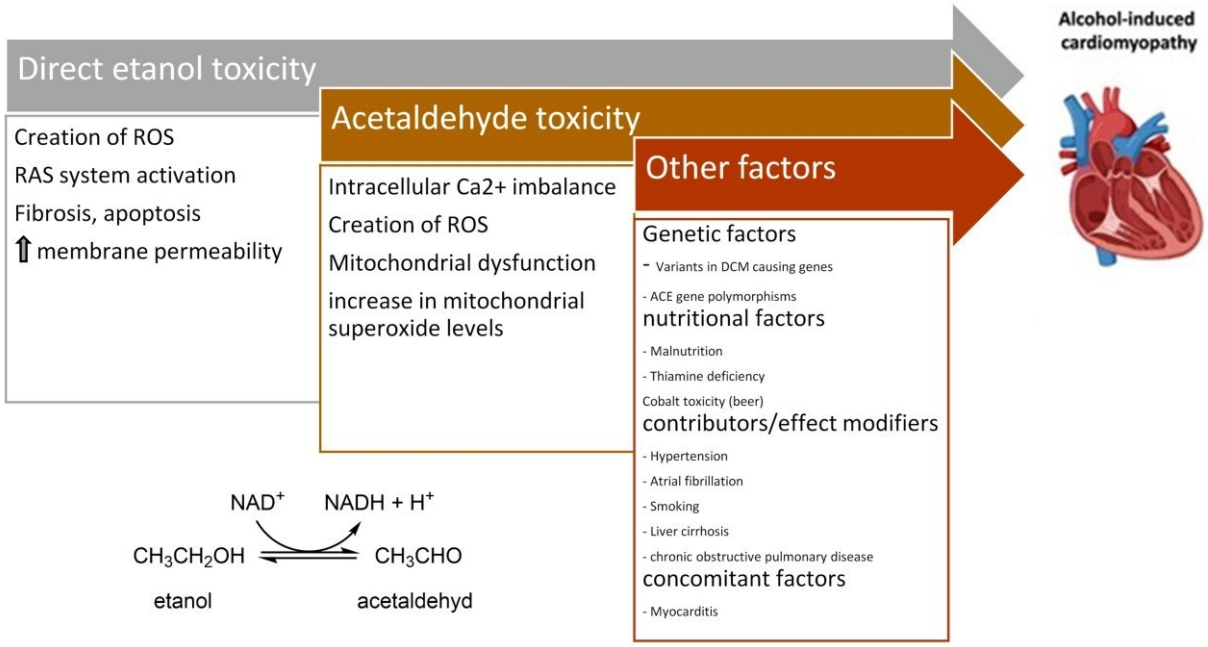

Figure 1: Pathogenic mechanisms of alcohol-induced cardiomyopathy. ACE, angiotensinconverting enzyme; DCM, dilated cardiomyopathy; RAS, renin–angiotensin system; ROS, reactive oxygen species.

1.3.2 Diagnosis of Alcoholic Cardiomyopathy

Initial symptoms in AC include acute shortness of breath, orthopnea, and paroxysmal nocturnal dyspnea. Symptoms of low cardiac output, such as fatigue and weakness, can also be observed. Over time, signs of right-sided heart failure, including edema, jugular venous distension, and hepatomegaly, may develop. Jugular venous pressure can assist in differentiating cirrhosis in these patients,

particularly in the absence of tense ascites, which can elevate the intrathoracic pressure.[29]

The definition of AC includes heavy alcohol consumption of more than 80 g/day over at least 5 years. Additionally, it is characterized by a left ventricular end-diastolic diameter greater than 2 standard deviations above normal, along with an LVEF of less than 50%. Other potential causes of heart failure, such as hypertensive, valvular, and ischemic heart disease, must be excluded. Addiotional possible signs are increased levels of Nt-pro-BNP and/or liver enzymes (alanine aminotransferase and aspartate aminotransferase), macrocytosis, anaemia, folate and vitamin B12 deficiency, thrombocytopenia, hypertriglyceridaemia, hyperuricaemia, hypoalbuminaemia and electrolyte imbalances.[29], [32], [33]

1.3.2.1 Echocardiographic changes in Alcoholic Cardiomyopathy

AC has no pathognomonic signs to differentiate it from an idiopathic dilated cardiomyopathy (iDCM). Typically, it comes with a left ventricular dilation and impaired systolic function. These changes are mostly already subclinically present. [34]

Other echocardiographic changes have been explored in more recent studies. They desribed not only an increased left ventricular end-diastolic volume but also a decreased E/A ratio and a prolonged isovolumic relaxation time have been desribed.[35], [36]

Furthermore, other studies have also shown a decrease in the left ventricular global longitudinal strain (LVGLS) and left ventricular global circumferential strain in alcohol abusers.[29], [37]

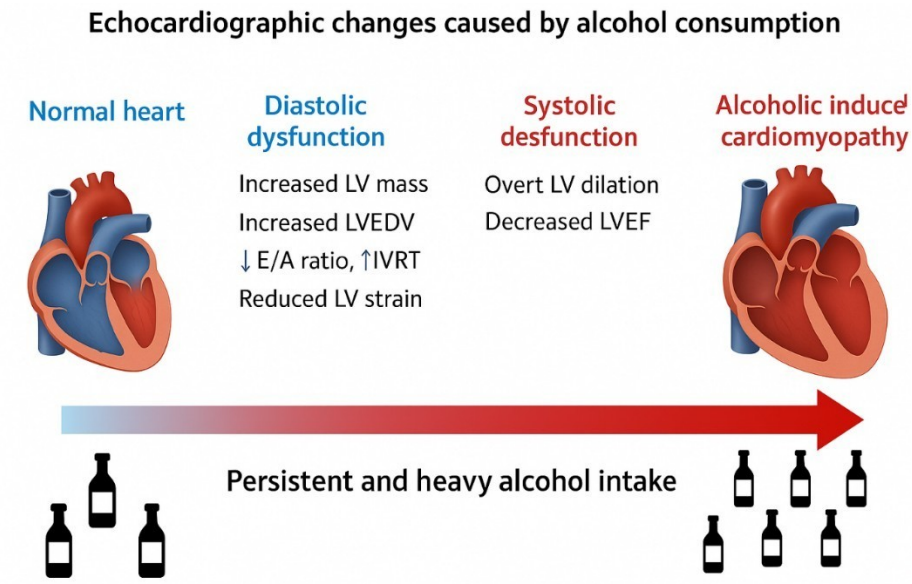

Figure 2: Echocardiographic consequences of heavy and persistent alcohol consumption. IVRT, isovolumic relaxation time; LVEDV, left ventricular end-diastolic volume; LVEF, left ventricular ejection fraction.

1.4 Toulouse Algorithm

The Toulouse Algorithm is based on a prospective study investigating predictive factors for cardiac decompensation after a TIPS in cirrhotic patients. The study included 174 cirrhosis patients who received TIPS between 2011 and 2016, but only 100 patients who underwent a full cardiac evaluation were analyzed. The assessments involved standard biological parameters, transthoracic echocardiography, and right heart catheterization, and patient follow-up was one year after the procedure. The primary endpoint was the incidence of cardiac decompensation requiring hospitalization.[13]

20% of the patients experienced cardiac decompensation within one year following TIPS. Several factors were associated with an increased risk of severe decompensation, including a prolonged corrected QT interval, elevated pre-TIPS brain natriuretic peptide (BNP) or NT-proBNP levels, elevated E/A ratio, elevated E/e′ ratio, elevated LAVI and the presence of aortic stenosis. The study found that a BNP level <40 pg/mL and NT-proBNP level <125 pg/mL indicated a low risk for cardiac decompensation. Additionally, the absence of diastolic dysfunction in echocardiography is a sign of a low risk for decompensation. The Toulouse

Algorithm combines the BNP/NT-proBNP levels and echocardiographic parameters (LAVI, E/e', and E/A) to stratify patients into a zero, low and high risk group. This algorithm should help to improve patient selection for TIPS procedure and predict the risk of cardiac decompensation in these patients.[13]

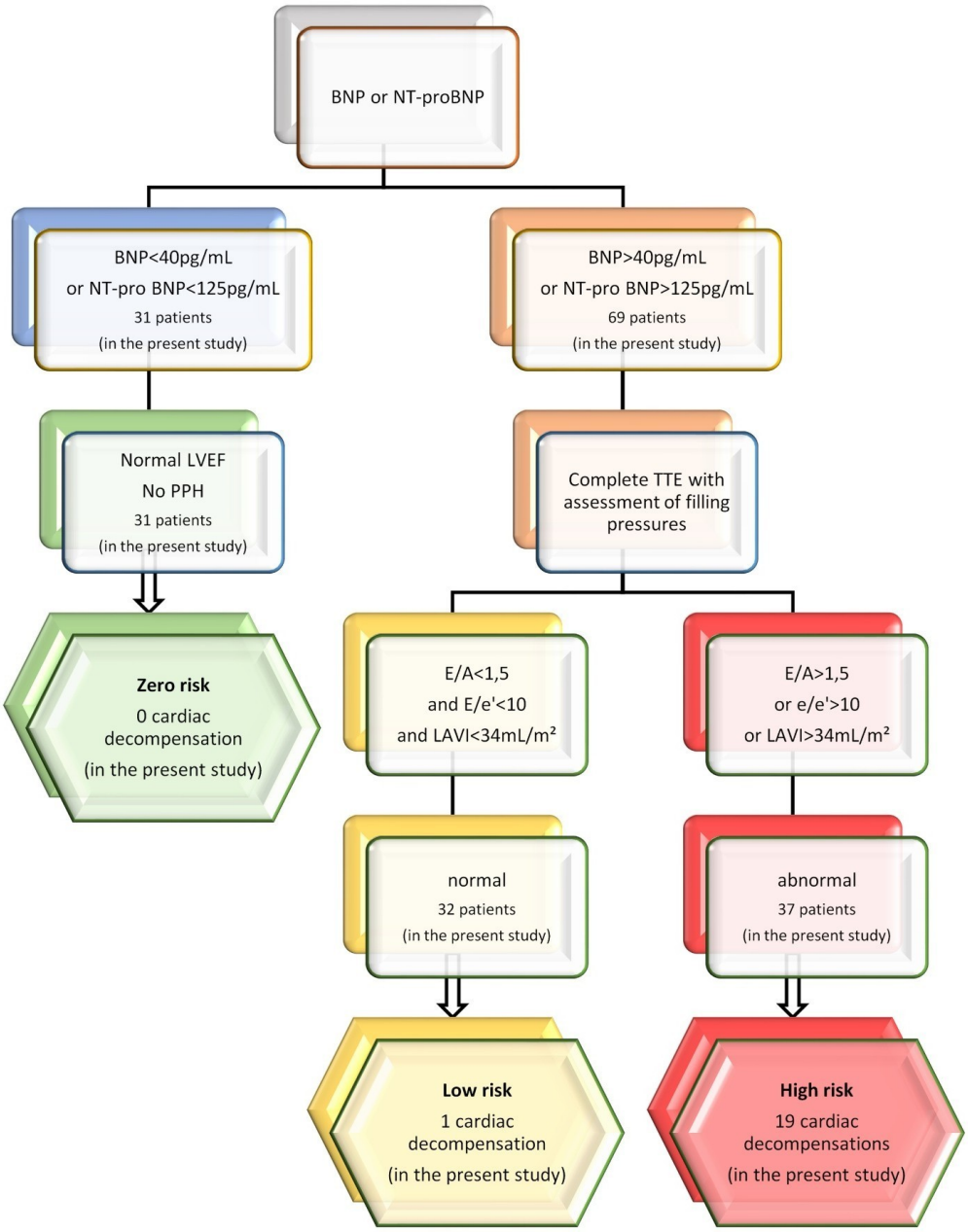

Figure 3: The Toulouse algorithm for patient selection regarding the risk of post-TIPS cardiac decompensation.BNP, brain natriuretic peptide; NT-pro BNP, N-terminal pro-brain natriuretic peptide; TTE, transthoracal echocardiography; LVEF, left ventricular ejection fraction; LAVI, left atrial volume index; PPH, porto-pulmonary hypertension.

1.5 Transthoracic Echocardiography

TTE is a non-invasive imaging modality that delivers crucial data on cardiac function, which is essential for managing patients with various conditions and diagnosing a range of diseases. [38]

The concept of ultrasound examination was first introduced by Lazzaro Spallanzani in the 18th century, when he described the reflection of inaudible sound waves. In 1954, Hertz and Edler pioneered the use of ultrasound for cardiac evaluation, using an industrial ultrasonic flaw detector to monitor heart movements and obtain timevarying echoes. The first clinical application of echocardiography was the examination of the mitral valve with M-mode. Since then, echocardiography has seen tremendous growth and has become an essential tool in cardiac evaluation. [39], [40], [41], [42]

Echocardiography initially relied on B-mode, but with the development of new technologies such as Doppler and 3D imaging, the echocardiographic examination has become increasingly detailed and comprehensive over time. [43], [44]

1.5.1 Mechanisms and Techniques of Echocardiography

1.5.1.1 Ultrasound Physiology

Echocardiographic probes use ultrasound waves with frequencies ranging from 1.5 to 7.5 MHz. The speed of these waves varies depending on the component they travel through, with sound traveling at 330 m/s in air and around 1540 m/s in heart tissue. Ultrasound waves are generated by converting electrical oscillations into sound waves. When the sound waves are reflected, the probe's crystal converts them back into electrical signals, a process known as the piezoelectric effect. Each probe contains a piezoelectric crystal transducer that vibrates under different voltages to emit ultrasound waves. The probe sends sound waves to the body, and the tissues reflect these waves back to the probe. When the waves are reflected, the transducer produces an electrical signal that is interpreted by the ultrasound scanner. The distance to the tissue is calculated using the speed of sound in that tissue and the time it takes for the echo to return. A two-dimensional image is created by displaying the intensity of the echoes and the calculated distances.[45]

1.5.1.2 M Mode

Ultrasound waves are sent along a single line and the reflected signal's amplitude and depth are displayed on an oscilloscope. Plotting these signals over time producs M-mode images. While 2D and 3D imaging are more common today, M-mode remains valuable due to its high sampling rate and excellent temporal resolution. [38].

The M-mode images are presented as graphs, with time on the x-axis and distance from the transducer on the y-axis. Structures closer to the transducer appear at the top of the image.[29]

TAPSE (Tricuspid Annular Plane Systolic Excursion) is a simple and valuable measurement used to assess right ventricular systolic function. It measures the systolic excursion of the tricuspid annulus and is typically performed using the Mmode in the apical 4-chamber view.

The resulting M-mode image will display the movement of the tricuspid annulus during systole and diastole.

TAPSE provides a direct measure of the right ventricular systolic function. It quantifies how much the tricuspid annulus moves toward the heart apex during systole, which correlates with the contractile ability of the right ventricle. A normal TAPSE value indicates that the right ventricle is contracting effectively, whereas a reduced TAPSE suggests impaired right ventricular function.

1.5.1.3 2D Echocardiography

2D echocardiographic imaging offers tomographic views of the heart from different planes and serves as a guide for M-mode and Doppler echocardiography. In 2D imaging, instead of using a fixed scan line, the ultrasound beam sweeps across an arc. The echocardiographic machine then processes the data from multiple scan lines to generate a 2D tomographic image for display.[39]

1.5.1.4 Doppler Imaging

The introduction of Doppler to 2D echocardiography added the ability to assess blood flow dynamics non-invasively. The Doppler principle measures frequence shifts caused by moving blood cells, which helps calculate their velocity using the Doppler equation. For accurate velocity measurements, the angle between the ultrasound beam and blood flow should be as close to zero as possible, ideally under 20°. Doppler imaging is displayed through spectral analysis and includes Pulsed Wave (PW) Doppler and Continuous Wave (CW) Doppler. PW Doppler measures velocity at specific locations using short ultrasound bursts, but is limited in measuring high velocity flow by aliasing. CW Doppler, on the other hand, continuously transmits and receives ultrasound waves, making it ideal for measuring high-velocity flow without aliasing. PW Doppler is used for measuring flow in specific areas, while CW Doppler is used for measuring maximal velocities.[29], [40]

1.5.1.4.1 Pulse-wave Doppler

The E- and A-waves are essential components of the mitral inflow velocity curve, which is typically assessed using Pulsed-Wave Doppler (PW Doppler) positioned at the mitral valve tips in the A4C view. This view allows precise assessment of blood flow from the left atrium to the left ventricle. The resulting Doppler spectrum will display two primary peaks, which represent different phases of ventricular filling during diastole. The analyze of these waves are crucial for evaluating diastolic function and diagnosing diastolic dysfunction.

The E-wave represents early ventricular filling and is primarily influenced by ventricular relaxation and ventricular compliance. In a healthy heart, the E wave is typically the dominant component of the mitral inflow pattern. A reduced E-wave velocity may indicate impaired ventricular relaxation, commonly observed in conditions like diastolic heart failure or hypertensive heart disease.

The A-wave corresponds to atrial contraction, reflecting the atrial contribution to ventricular filling. An increased A wave suggests decreased ventricular compliance, as the atrium must work harder to push blood into the ventricle. In cases of diastolic

dysfunction, the A-wave may become more prominent, reflecting an increased reliance on atrial contraction for filling, particularly when the ventricle is stiff and less compliant.

The E/A ratio, which compares the velocities of the E and A waves, is another tool to assess the diastolic function. In a normal heart, the E-wave is greater than the Awave, resulting in an E/A ratio greater than 1. However, in patients with diastolic dysfunction, the ratio may decrease, or the A-wave may become larger than the Ewave, leading to a ratio less than 1. Due to increased filling pressures especially in the left atrium, the E/A ratio gets greater than 1 in conditions of severe diastolic dysfunction again.

Tissue doppler imaging

To measure e′ (e prime) using Tissue Doppler Imaging (TDI), also the apical 4chamber view is typically used. e′ (early diastolic velocity) is the velocity of the mitral annulus during early diastole, reflecting the rate of ventricular relaxation. It is an important measure of the diastolic function of the left ventricle. A decrease in e′ typically indicates impaired diastolic relaxation, which may be seen in conditions such as diastolic heart failure, hypertensive heart disease, or restrictive cardiomyopathies. The measurement of e′ represents an important component of the assessment of the diastolic function.

s′ (s prime) is another measurement in TDI, particularly when evaluating systolic function of the heart. It represents the systolic velocity of the mitral or tricuspid annulus and reflects the longitudinal systolic function of the left or right ventricle, respectively.

Continuous Doppler

TRVmax (Tricuspid Regurgitant Velocity Maximum) is a crucial measurement used to estimate the systolic pulmonary artery pressure. This velocity is typically measured in meters or cm per second (cm/s; m/s) and is an important indicator of the pressure gradient between the right ventricle and the right atrium. TRVmax is directly related to the right ventricular systolic pressure and, indirectly, to the

pulmonary artery pressure. A normal TRVmax is typically less than 2.8 m/s, which suggests a normal systolic right ventricular pressure or normal systolic pulmonary artery pressure. Higher TRVmax values can be a hint for elevated pulmonary artery pressures.

1.6 Echocardiographic views

1.6.1 Parasternal long axis view

The parasternal long-axis view (PLAX) is one of the standard transthoracic echocardiographic imaging planes, obtained by placing the ultrasound transducer on the left side of the sternum, typically in the third or fourth intercostal space. The probe is oriented in a parasagittal plane, angled slightly toward the right shoulder. This view allows for a longitudinal section of the heart and provides detailed visualization of several key cardiac structures, including the left ventricle, right ventricular outflow tract, interventricular septum, posterior (inferolateral) wall, left atrium, mitral valve, aortic valve, and proximal ascending aorta.

1.6.2 Apical four chamber view

The four chamber view (A4C) is a standard echocardiographic imaging plane obtained by placing the transducer at the apex of the heart, typically in the left fifth intercostal space. The probe is oriented to visualize both the left and right atria and ventricles in a single cross-sectional image.

1.6.3 Apical two chamber view

The apical two-chamber view (A2C) is an echocardiographic imaging plane obtained by positioning the ultrasound probe at the apex of the heart, typically in the left fifth intercostal space. The probe normally lies approximately 90 degrees in relation to the position in the A4C view. It enables the visualization of the left atrium and left ventricle in a longitudinal view.

1.6.4 Apical three chamber view

This view is gathered from the apical window, with the probe rotated ~120° from the standard A4C-view. It provides important information about left ventricular function, aortic valve morphology, and mitral valve function.

1.6.5 Subcostal view

The Inferior Vena Cava (VCI) diameter is an important measurement in echocardiography used to assess right atrial pressure and fluid status in patients.

The size of the VCI, particularly its diameter, is influenced by the right atrial pressure, venous return, and overall fluid balance. Changes in the VCI diameter can provide valuable information about right heart function, venous congestion, and even help in the assessment of volume status in critically ill patients. It is also important to observe collapsibility during respiration, as the VCI collapses with inspiration in patients with normal right atrial pressure and increased compliance. In contrast, a non-collapsing or poorly collapsing VCI suggests elevated right atrial pressure and increased central venous pressure.

1.7 Aim of the Thesis

Currently, there is a significant lack of existing literature on the topic of alcoholic cardiomyopathy, with little information available regarding the cardiac risks associated with TIPS. Many potential parameters have not been tested for their ability to predict cardiac decompensation or acute heart failure in this patient population.

The aim of this study is to identify echocardiographic predictors for cardiac decompensation or acute heart failure in patients after the implantation of a TIPS. Additionally, the study seeks to evaluate the efficacy of the Toulouse algorithm in relation to the echocardiographic parameters as a decision-making tool for risk assessment prior to the TIPS procedure.

2. Methods

The data for this diploma thesis was obtained from a prospective database maintained by the Department of Hepatology in Graz. This database includes all patients who underwent a TIPS procedure at the University Hospital Graz between 2004 and 2024. 74 Patients with echoloops were included in the present analysis.

2.1 Study Overview and Study Population

The prospective single-center registry conducted at the Division of Hepatology, Department of Internal Medicine, Medical University Graz includes data from 244 patients who underwent a TIPS procedure between 2004 and 2024. It contains detailed information on the patients` demographics and clinical characteristics, indications for TIPS placement, procedural details, potential complications, followup assessments, as well as laboratory findings and other diagnostic investigations. For the primary analysis of this diploma thesis, the database was retrospectively reviewed with a specific focus on patient‘s echocardiographic parameters. Ethical approval for the study was granted by the Ethics Committee of the Medical University of Graz (EK Nr: 1212/2025).

An in-depth echocardiographic analysis was performed using a vendor-independent post-processing software as described in section „Transthoracic Echocardiography“.

The focus of this analysis was on cardiac chamber dimensions, left and right ventricular function, as well as diastolic function. Patients were stratified into low- and high-risk groups based on echocardiographic parameters defined by the Toulouse Algorithm. In addition, cardiac outcomes were evaluated, with particular attention to identifying patients who developed clinical signs of cardiac decompensation within one year post-procedure.

2.2 Transthoracic Echocardiography

All image data was analyzed retrospectively, using the post-processing program TomTec (TOMTEC Imaging Systems, Munich, Germany) in digitally saved, ECG triggered 2D TTE. To ensure accuracy and minimize potential measurement errors, each parameter was assessed twice during separate cardiac cycles, if available. All measurements were obtained from standard echocardiographic views including the parasternal long-axis view (PLAX), the apical four chamber view (A4C), the apical two chamber view (A2C) and the apical three chamber view (A3C) as well as the subcostal view, which was utilized to evaluate venous filling pressures. Additionally, PW Doppler, Tissue Doppler Imaging, M-Mode, and CW Doppler were utilized to obtain further parameters for a more comprehensive assessment of cardiac function. The parameters were assessed based on the availability and quality of the respective recorded echocardiographic images.

2.2.1 Parasternal Long Axis View

In this study we used the parasternal long axis view (PLAX) view to analyze the dimensions of the interventricular septum (IVSed), the posterior wall thickness (PWed), the left ventricular diameter (LVEDD) end diastolic, and the left atrial diameter (LA_diameter) end systolic. All parameters were meassured according tot he latest guidlines and recorded in millimeters (mm).

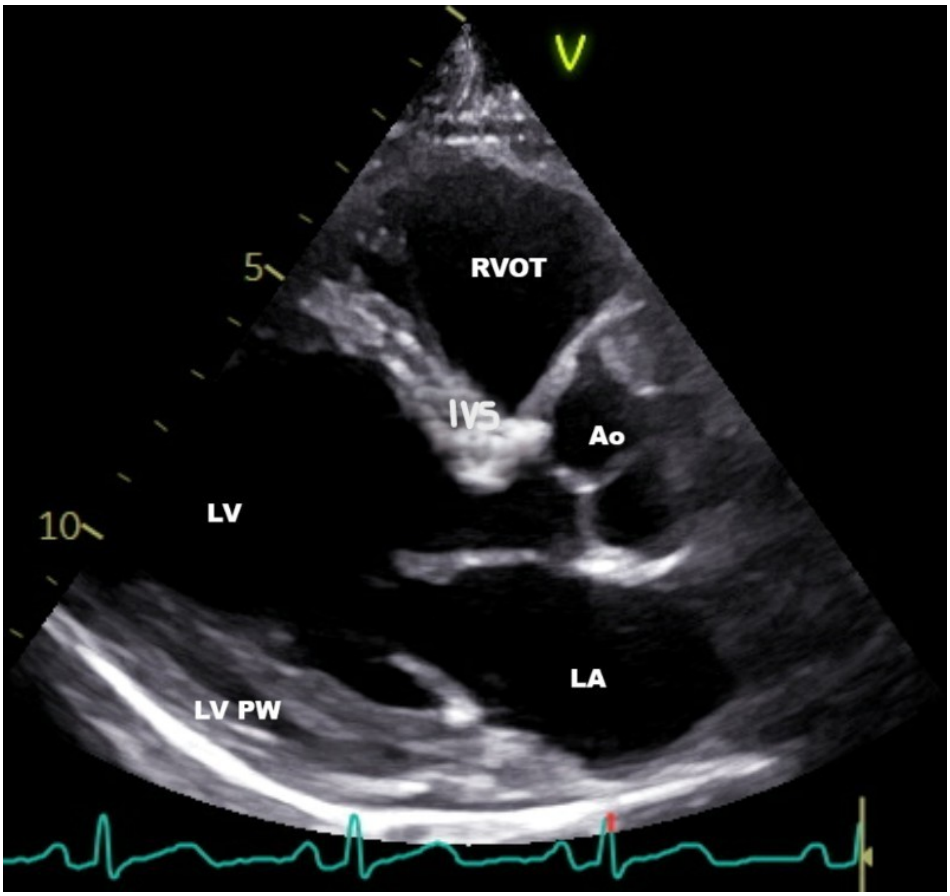

Figure 4: Parasternal long axis view. RV, Right ventricle; RVOT, Right ventricular outflow tract; LV, Left ventricle; LV PW, Left ventricular posterior wall; LA, Left atrium; AO, Aorta; IVS, Interventricular septum

2.2.2 Apical four chamber view

For this study, we analyzed several parameters in the apical four-chamber view. The volumes of the left ventricle end diastolic (LVEDV) and end systolic (LVESV), measured in cubic centimeters (cm^3), were assessed. Using the Simpson's approach, these parameters, along with those obtained from the apical two-chamber view, were used to calculate the left ventricular ejection fraction (LVEF).

Furthermore, the parameters of both atria with the left and right atrial volumes at end-systole (LAarea_ES/RAarea_ES) in cm^3, and the maximal lengths at endsystole (LAlength_ES/RAlength_ES) in mm were measured. The right atrial volume (RAV_ES) was calculated using these two areas, while for the left atrial volume (LAV_ES), both end-diastolic and end-systolic areas from the apical two-chamber view were incorporated for the biplane calculation.

For further calculations, the right atrial volume index (RAVI) was also assessed, utilizing the body surface area (BSA) for normalization. Additionally, the left atrial strain was also evaluated with the three parameters LASr, LAScd, and LASct, expressed as percentages (%).

Regarding the right ventricle, the basal diameter (RVEDD_basal), mid-diameter (RVEDD_mid), and maximal length (RVEDL) in mm, as well as the end diastolic (RVAd) and end systolic areas (RVAs) in cm², were measured. These measurements were used to calculate the fractional area change (RVFAC), expressed in %. Furthermore, the strain of the right ventricle was evaluated with the parameters right ventricular free wall longitudinal strain (RVFWSL) and right ventricular four-chamber longitudinal strain (RV4CSL), also expressed as %. Finally, the interventricular septum (IVSed), posterior wall thickness (PWed), and left ventricular end-diastolic diameter (LVEDD) were re-measured in this view.

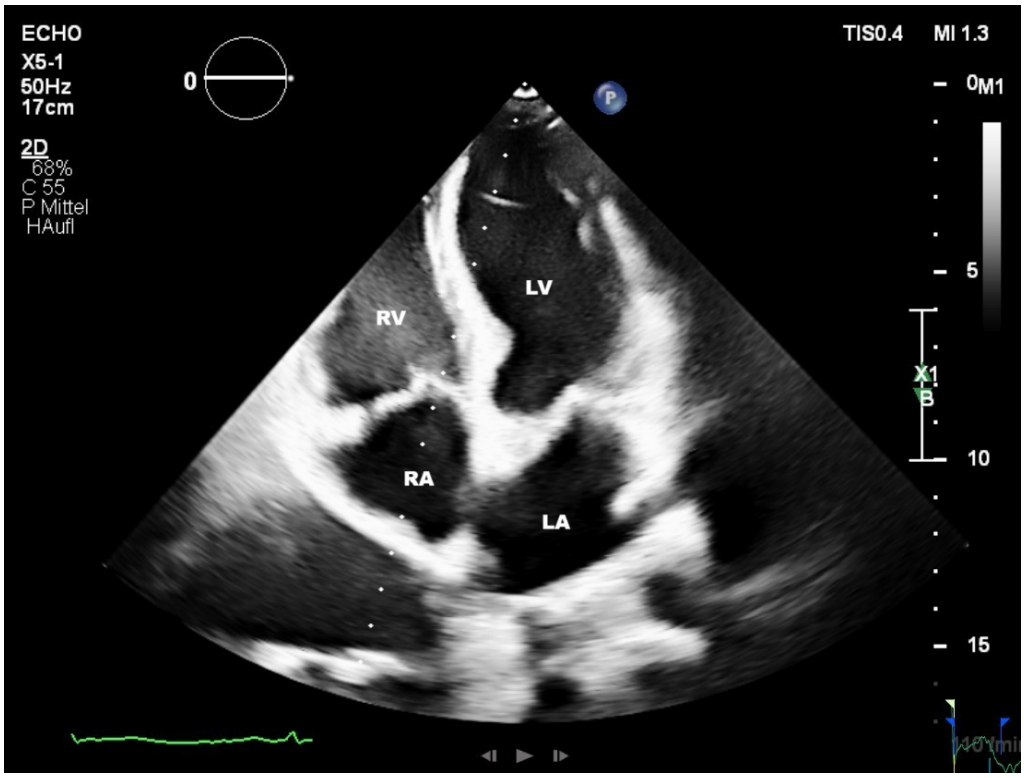

Figure 5: Apical four chamber view. LV, Left ventricle; RV, Right ventricle; LA, Left atrium; RA, Right atrium; MV, Mitral valve; TV, Tricuspid valve

The E- and A-waves were assessed by using the Pulsed-Wave Doppler. The PW Doppler got positioned at the mitral valve tips in the A4C view. The two primary

peaks, which represent the E- and A-wave, were analyzed and the ratio E/A was calculated.

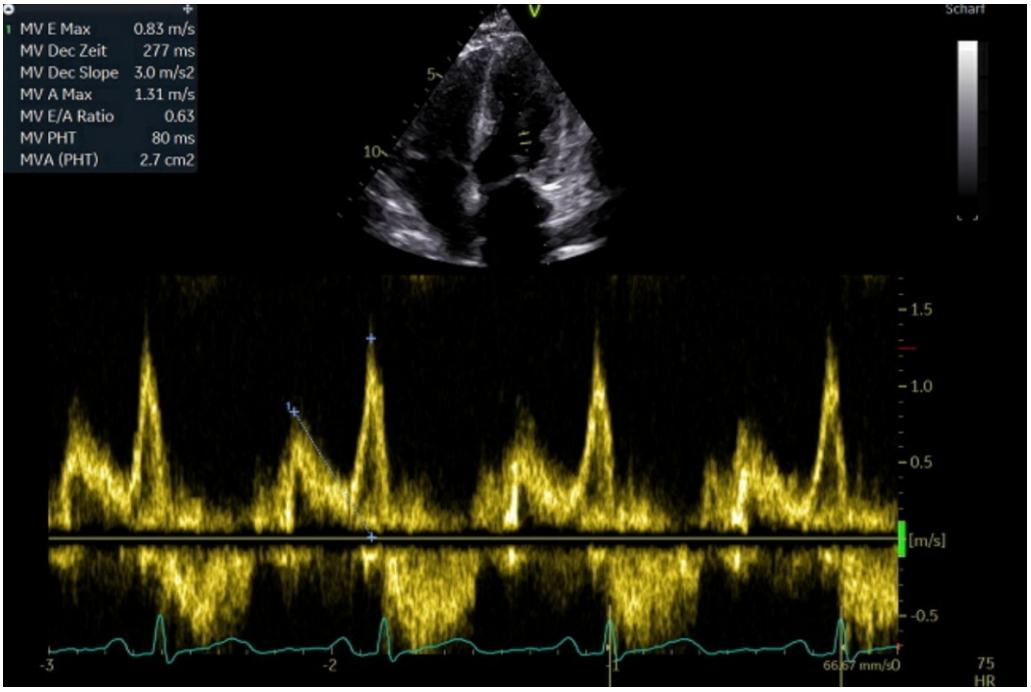

Figure 6: E- and A-wave in a pulse-wave Doppler view; Example of a patient with a diastolic dysfunction with an E/A ratio of 0.63; MV, mitral valve; E Max, maximal velocity oft he E wave; Dec Zeit, deceleration time, Dec Slope, deceleration slope, A Max, maximal velocity oft he A wave; MV PHT, Mitral Valve Pressure Half Time, MVA (PHT), Mitral Valve Area by Pressure Half Time; HR, heart rate

With the help of the tissue doppler imaging (TDI) the e′ medial and lateral could be measured. In the A4C view, the doppler sample volume is placed at the mitral annulus, once at the septal and once at the lateral side. When performing the TDI, the resulting waveform will show multiple velocities corresponding to different phases of the cardiac cycle. Also s′ (s prime) was analyzed using the TDI.

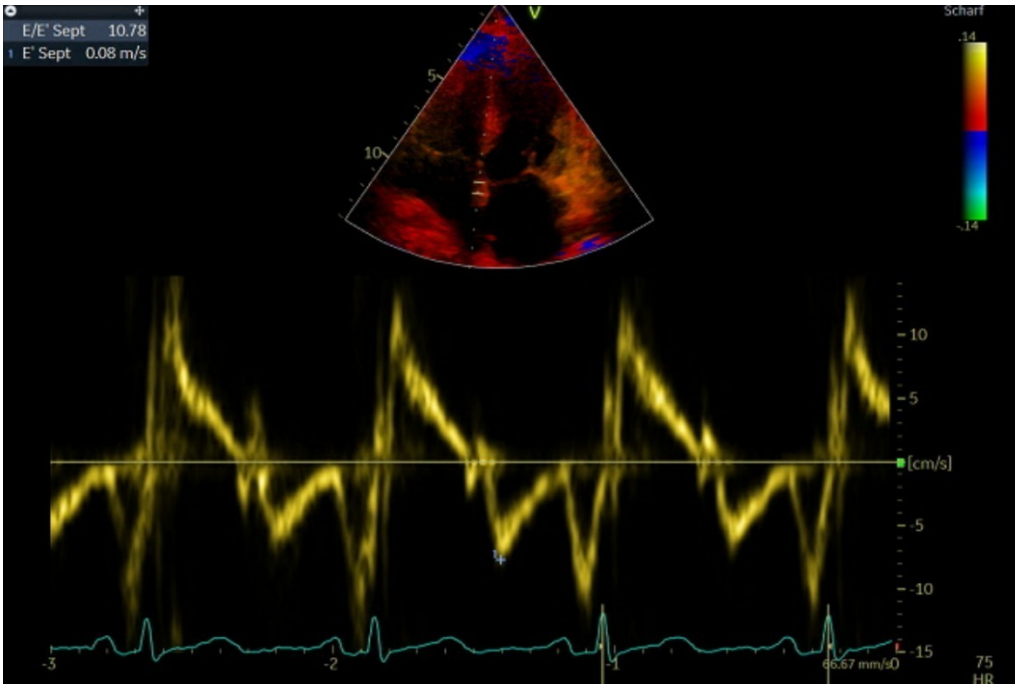

Figure 7: Example of the measurement of E' Septal; here is E' Septal 10.78cm/s; E' Sept, E prime septal; E/E' Sept, Ratio of E to E prime septal

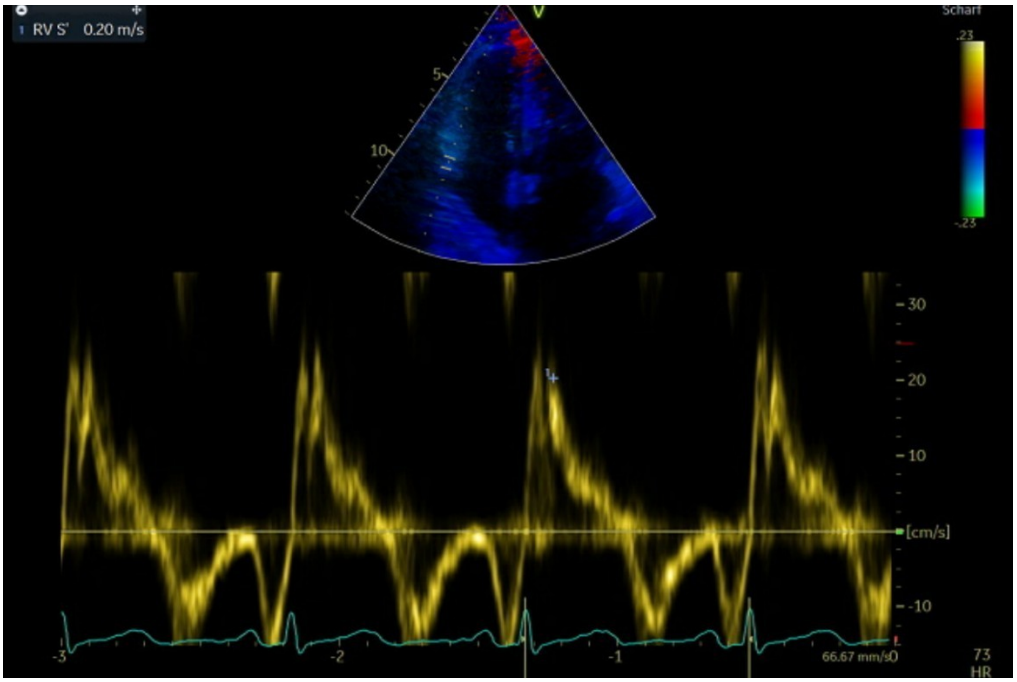

Figure 8: Example of the measurement of S'; in this case S' is 0.20m/s; RV S', right ventricular S prime

TAPSE is defined as the peak systolic excursion of the annulus, measured from its position at end-diastole to its farthest point during systole while using the M-Mode. This movement reflects the longitudinal contraction of the right ventricle.

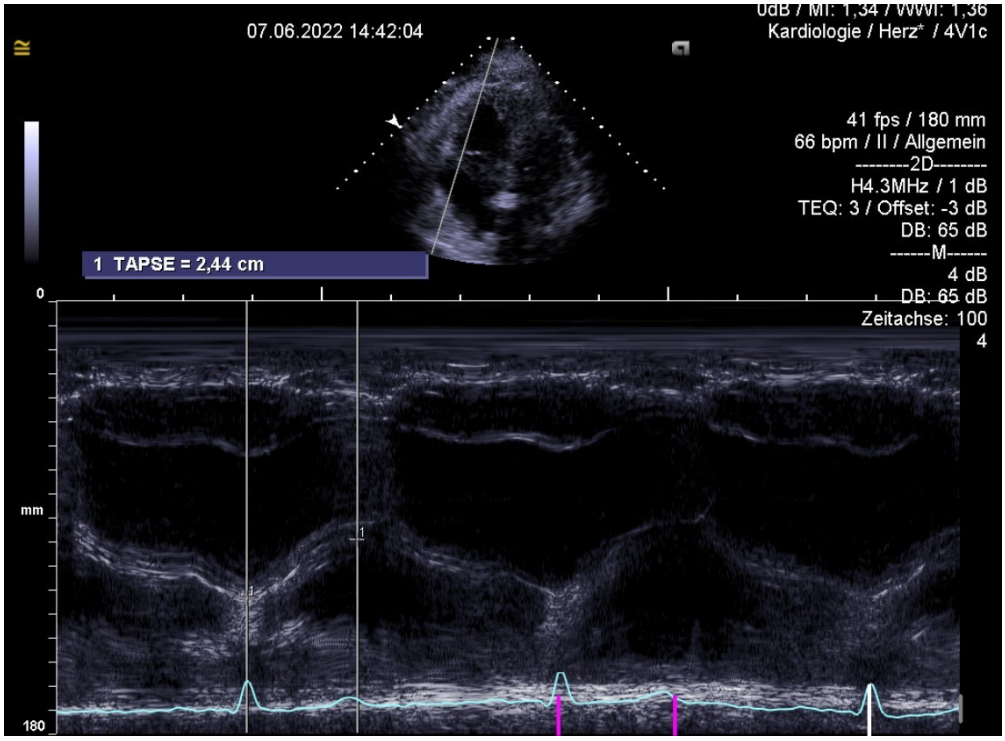

Figure 9: Example of the measurement of TAPSE in the M-Mode, in this case TAPSE is 2.44cm; TAPSE, Tricuspid Annular Plane Systolic Excursion

To measure TRVmax, the CW Doppler is placed just below the tricuspid valve to capture the high-velocity flow of blood as it regurgitates into the right atrium. The TRVmax is then recorded as the maximum velocity of the tricuspid regurgitant jet, which corresponds to the peak of the Doppler waveform during systole.

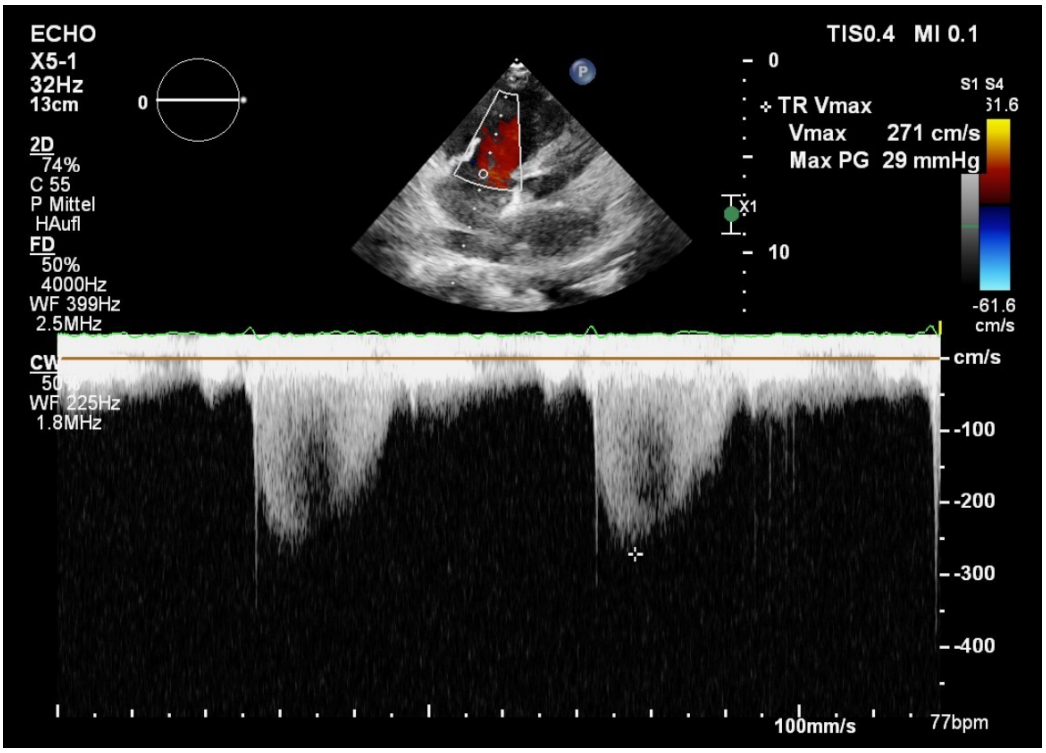

Figure 10: Example of the measurement of TRVmax in the continous Doppler view; TRVmax is in this case 2,71m/s; TR Vmax, Tricuspid Regurgitant Velocity Maximum; Max PG, maximum pressure gradient

2.2.3 Apical two chamber view

In this study we measured the left ventricular end-diastolic (LVEDV_A2C) and endsystolic volume (LVESV_A2C) in cm^3, which allowed, as previously mentioned, the calculation of the biplane left ventricular end diastolic volume (LVEDV_biplane) and end systolic volume (LVESV_biplane) in cm^3, ultimately leading to the biplane left ventricular ejection fraction (LVEF) in percentage (%). The biplane LVEF was evaluated through TTE according to current European Society of Cardiology (ESC) guidelines, using the Simpson method. Additionally, the left atrial area (LAarea_ES_A2C) and the maximal length (LAlength_ES_A2C), both end systolic, were assessed to calculate the biplane end systolic left atrial volume (LAV_ES_biplane) in cm^3. Moreover, the left atrial volume index (LAVI) was calculated by normalizing the left atrial volume using the patient's BSA.

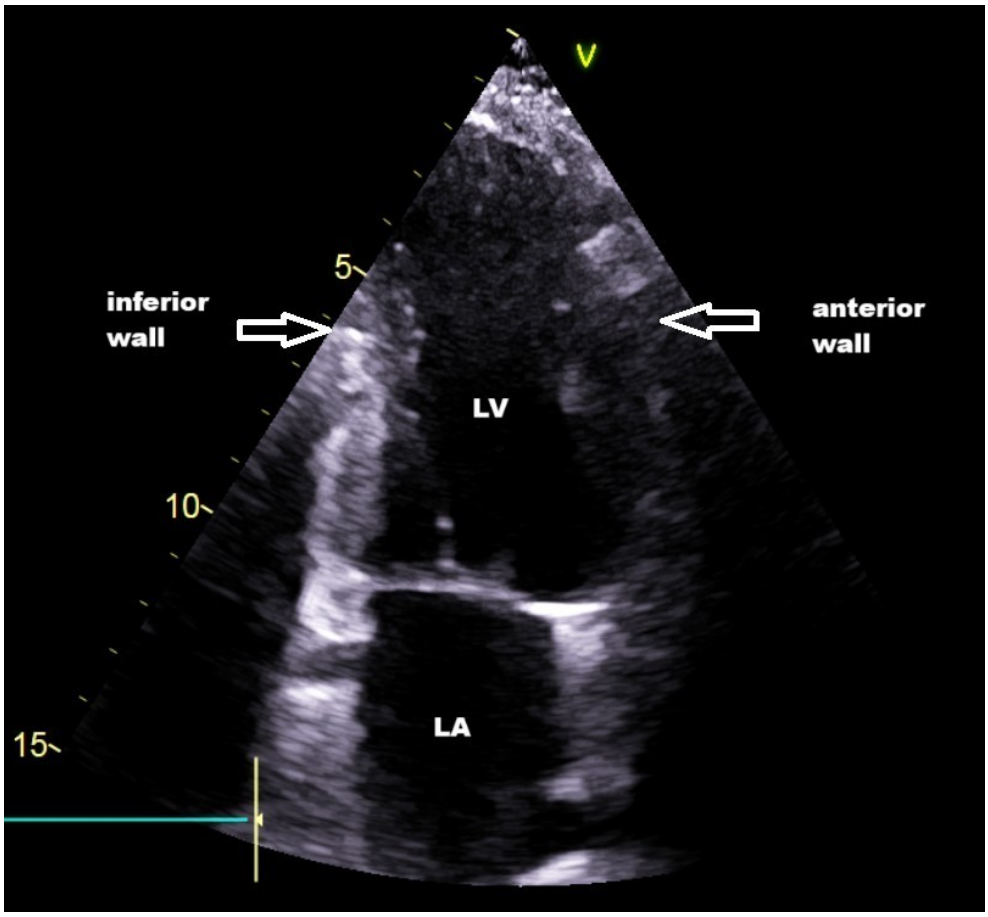

Figure 11: Apical Two Chamber View, LA=Left atrium, LV=Left ventricle

2.2.4 Apical three chamber view

In our study, the apical three chamber (A3C) view was required to assess the left ventricular area in an additional plane, enabling the calculation of the left ventricular global longitudinal strain (LVGLS).

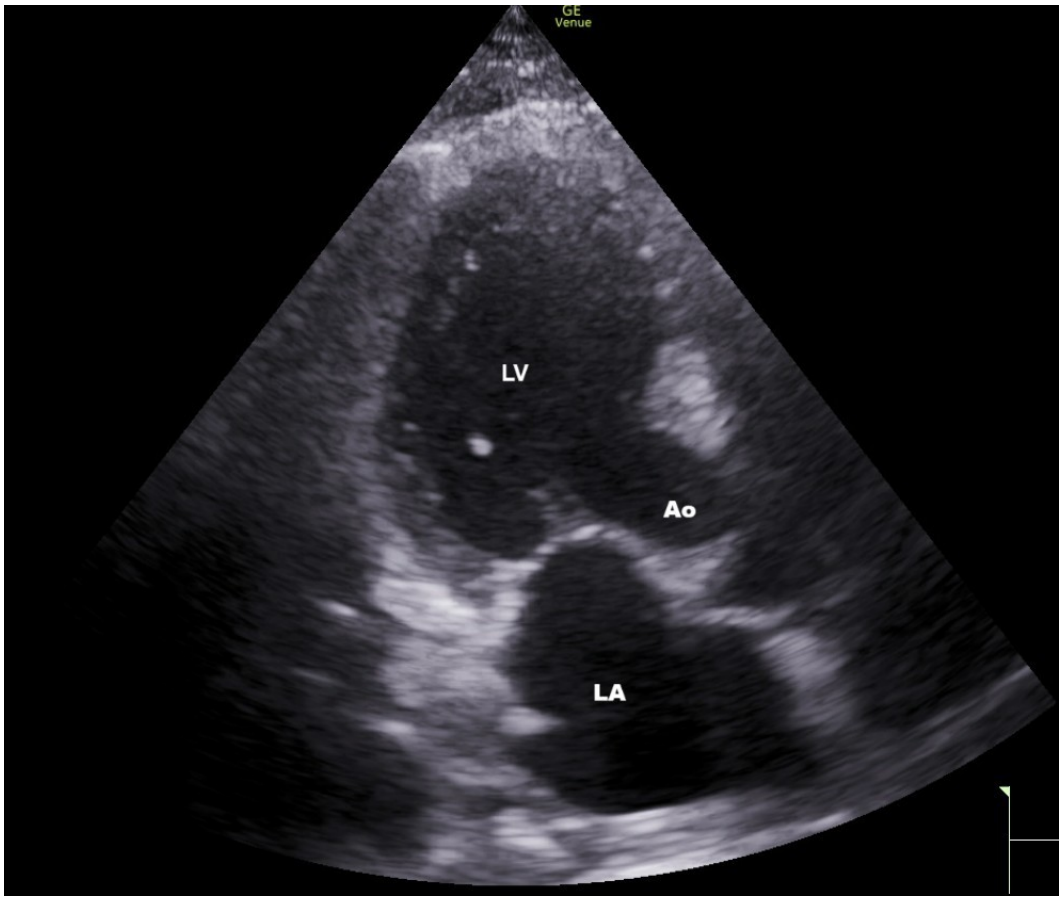

Figure 12: Apical Three Chmaber View, LA=Left Atrium, Ao=Aorta, LV=Left Ventricle[46]

2.2.5 AutoStrain

For our study the analyzing methode AutoStrain (TOMTEC Imaging Systems, Munich, Germany) was used. It is an automated tool used to assess the LVGLS along the endocardial border. After manually selecting the correct echocardiographic views (A4C, A2C and A3C), the software automatically traces the endomyocardial contours. These contours can be manually adjusted if necessary, with the option for re-tracking. We also used the AutoStrain to evaluate the left atrial and right ventricular strain.

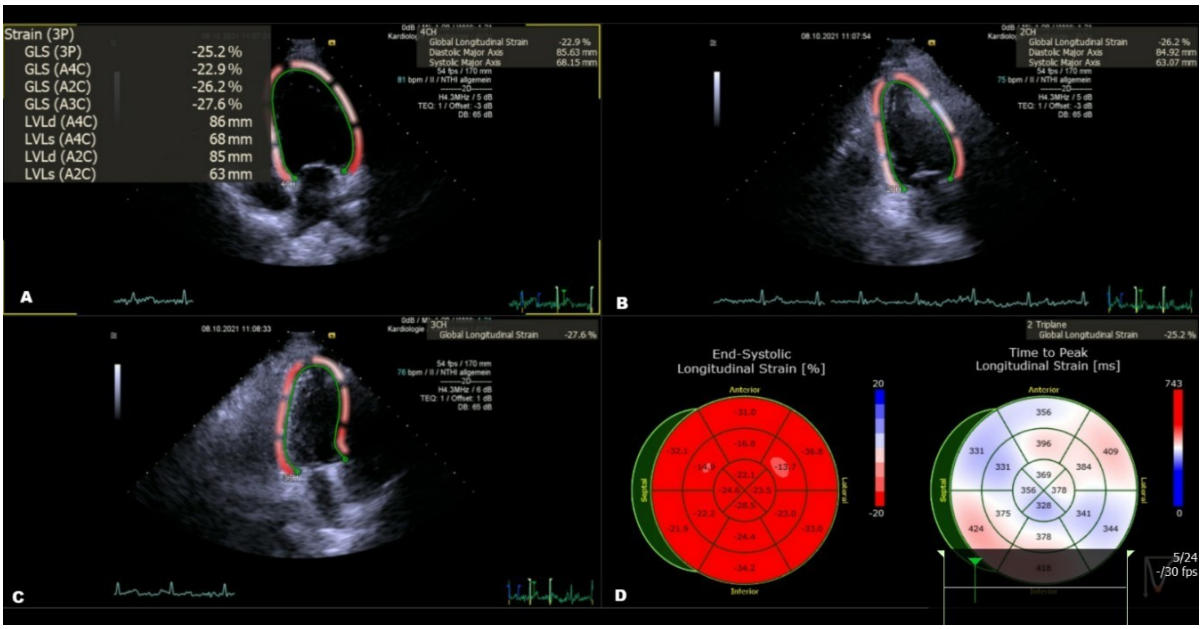

Figure 13: Example of an AutoStrain measurement using the software TomTec. Pictured was a patient with a GLS of -25.2%.
A: Apical four chamber view
B: Apical two chamber view
C: Apical three chamber view
D: Bull's eye plots for end-systolic [%] and time-to-peak Longitudinal Strain [ms]

2.2.6 Subcostal view

To measure the VCI diameter, the ultrasound probe is positioned in the subcostal view, which allows for clear visualization of the inferior vena cava as it enters the right atrium. In this view, the VCI is typically located just below the diaphragm, and the probe should be oriented to align the VCI in a longitudinal plane. The diameter of the VCI is measured at the level of its entrance into the right atrium, where it is the widest.

2.3 Risk stratification

Patients were stratified into two distinct risk categories: a low-risk group and a highrisk group. This stratification was based on echocardiographic parameters in accordance with the criteria of the Toulouse Algorithm (LAVI, E/e' and E/A).

The original Toulouse Algorithm integrades these parameters with natriuretic peptides, however, in this study, BNP and NT-proBNP values were excluded from the analysis due to limited availability of these laboratory measurements within the

dataset. Consequently, stratification was performed solely based on the echocardiographic parameters in two different groups.

Patients were assigned to the low-risk group if all of the following criteria were met:

- Left atrial volume index (LAVI) ≤ 34 mL/m²
- E/e′ ratio ≤ 10
- E/A ratio ≤ 1.5

Conversely, assignment to the high-risk group occurred if any one of the following thresholds was exceeded:

- LAVI > 34 mL/m²
- E/e′ ratio > 10
- E/A ratio > 1.5

2.4 Data analysis and statistics

Data was exported and cleaned in Excel (Microsoft Office 365, Microsoft Corporation, Redmond, USA). The cleaned data was then imported into IBM SPSS Statistics 26 (IBM Corporation, Armonk/New York, USA) for further statistical analysis. Results were considered statistically significant if the two-sided p-value was <0.05.

All data were tested for normal distribution and homogeneity of variance. Normal distribution was assessed visually and using the Shapiro-Wilk test. For group comparisons, an unpaired t-test was applied for normally distributed parameters, while the Mann-Whitney U test was used for parameters not meeting the normality assumption. Additionally, unpaired t-tests and ANOVA with Tukey-HSD post hoc multiple comparison tests were employed for group comparisons.

Correlation analysis for normally distributed parameters was performed using Pearson's Product-Moment Correlation, and Spearman's Rank-Order Correlation was applied for non-normally distributed data.

3. Results

The following paragraphs picture a summary of this study's outcomes. A complete list of all the results can be found in the appendix.

3.1 Subjects

A total of 74 patients were included in the study.

Table 2: Baseline characteristics, overall and stratified by risk.

		Overall N=74		Low risk (LAVI ≤ 34 mL/m², E/e' ≤ 10 and E/A ≤ 1.5) N=24		High risk (LAVI > 34 mL/m², E/e' > 10 or E/A > 1.5) N=32		p-value
		Data available n (%)	Median [interquartile range]	Data available n (%)	Median [interquartile range]	Data available n (%)	Median [interquartile range]	
Age		74 (100)	60 [53-67]	24 (100)	58 [52-65]	32 (100)	60 [55-69]	0.140
BMI,kg/m²		50 (68)	24,8 [22-30]	17 (71)	24,8 [23-30]	23 (72)	25 [22-29]	0.837
SBP, mmHg		25 (34)	116 [103-122]	10 (42)	119 [106-130]	11 (34)	107 [100-120]	0.291
DBP, mmHg		25 (34)	65 [57-70]	10 (42)	68 [61-77]	11 (34)	63 [55-69]	0.341
MAP, mmHg		26 (35)	81 [74-91]	11 (46)	88 [79-99]	11 (34)	74 [72-85]	0.052
MELD score		70 (95)	12 [10-19]	23 (96)	13 [11-19]	30 (94)	12 [11-17]	0.620
Female sex, n (%)	female	74 (100)	27 (37)	24 (100)	9 (38)	32 (100)	11 (34)	0.809
	male		47 (64)		15 (63)		21 (66)	
Etiology	Alcohol related	72 (97)	55 (75)	24 (100)	21 (88)	32 (100)	25 (78)	0.462
	Not alcohol related		17 (23)		3 (13)		7 (22)	
Indication for TIPS	Recurrend ascites	73 (99)	36 (49)	24 (100)	13 (54)	32 (100)	17 (53)	0.434
	Recurrend GI bleedings (>2x)		14 (19)		3 (13)		9 (28)	
	Active GI bleeding		14 (19)		5 (21)		5 (16)	
	other		9 (12)		3 (13)		1 (3)	
CHILD Score	A	59 (80)	5 (7)	19 (79)	0 (0)	27 (84)	4 (13)	0.294
	B		46 (62)		17 (71)		19 (59)	
	C		8 (11)		2 (8)		4 (13)	
Diabetes Mellitus	yes	74 (100)	23 (31)	24 (100)	5 (21)	32 (100)	10 (31)	0.388
	no		51 (69)		19 (79)		22 (69)	

Table 2: Baseline characteristics, overall and stratified by risk

Abbreviations: BMI, body mass index; TIPS, transjugular intrahepatic portosystemic shunt; RRsys, systolic blood pressure; RRdia, diastolic blood pressure; MAP, mean arterial pressure; MELD, Model for Endstage Liver Disease; AF, atrial fibrillation

3.1.1 Baseline Characteristics

Out of the 244 patients in the database, 74 met the criterias and were therefore included in the analysis. Of these, 49 patients had a transthoracic echocardiogram within six months prior to the TIPS procedure, 16 had one within six months after the procedure and 9 patients underwent a transthoracic echocardiogram both before and after the intervention.

The table provides a detailed overview of the baseline characteristics of patients, both overall and stratified by risk group. Based on these criteria, a total of 24 patients met the definition of the low-risk group, whereas 32 patients fulfilled the criteria for high-risk classification. 56 (75.7%) patients could be stratified into risk groups, 18 patients were not feasible for risk stratification due to limited availability of all required echocardiographic parameters.

The median age was 60 years (inter quartile range [IQR]: 53-67). In the low-risk group, the median age was 58 years (IQR: 52-65), while in the high-risk group, the median age was 60 years (IQR: 55-69). The youngest participant was a female with 31 years and the oldest one a male with 85 years. The gender distribution was 63% (n = 47) for males and 37% (n = 27) for females. Gender was equally distributed between risk groups (p = 0.140).

The median BMI was 24.8 kg/m² (IQR: 22-30). Both the low-risk and high-risk groups had similar median BMIs: 24.8 kg/m² (IQR: 23-30) versus 25 kg/m² (IQR: 22-29), respectively (p = 0.837).

The median systolic blood pressure (SBP) was 116 mmHg (IQR: 103-122). In the low-risk group, median SBP was slightly higher (119 mmHg, IQR: 106-130) compared to the high-risk group (107 mmHg, IQR: 100-120), but this difference was not statistically significant (p = 0.291). Similarly, the median diastolic blood pressure (DBP) in the low-risk group was slightly higher (68 mmHg, IQR: 61-77 mmHg) compared to the high-risk group (63 mmHg, IQR: 55-69).

The median mean arterial pressure (MAP) was 81 mmHg (IQR: 74-91) with a median MAP in the low-risk group of 88 mmHg (IQR: 79-99) and 74 mmHg (IQR: 72-85) in the high-risk group (p = 0.052).

23 (31%) had diabetes mellitus (DM). In the low-risk group, 5 (21%) patients had diabetes, while in the high-risk group, 10 (31%) had diabetes (p = 0.388).

3.1.2 Etiology an Indication for TIPS

The etiology of the liver disease is a critical factor influencing the course of disease and treatment outcomes in patients undergoing a TIPS procedure. In this cohort of 74 patients, the majority of patients had alcohol-related liver disease, with 55 patients (75%) being diagnosed with alcohol-related cirrhosis. The distribution of alcohol-related liver disease between the risk groups was as follows: 21 patients (88%) in the low-risk group and 25 patients (78%) in the high-risk group. These findings highlight the predominance of alcohol-related liver disease in both groups.

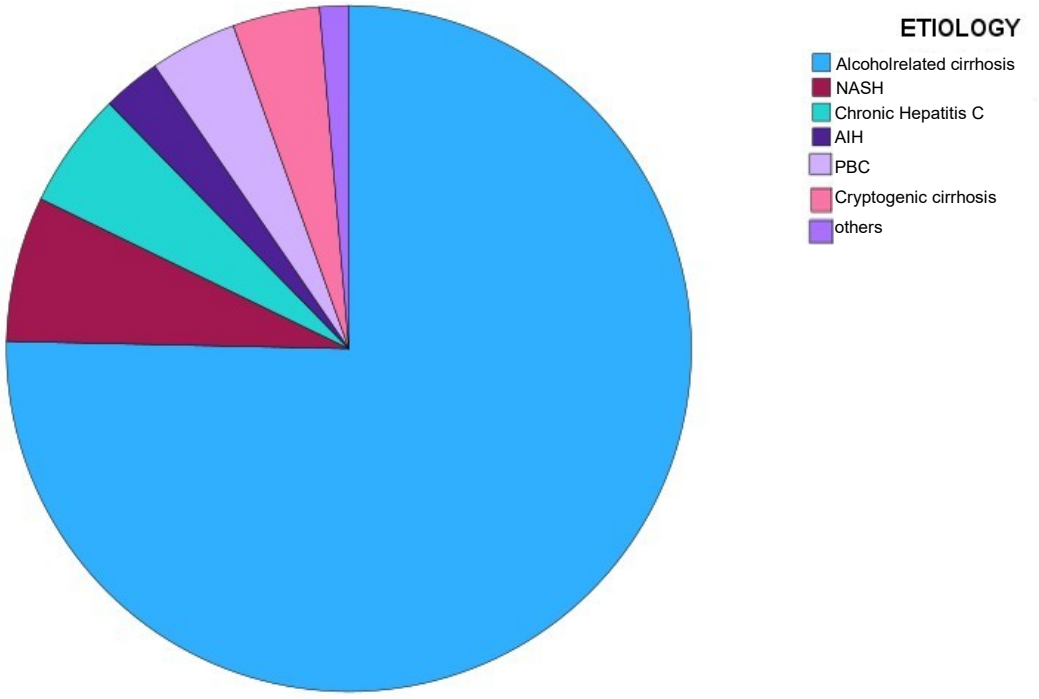

Figure 14: Distribution of TIPS Etiology

Abbreveations: NASH, non-alcoholic steatohepatitis; AIH, aotuimmune hepatitis; PBC, primary biliary cirrhosis

The decision to perform a TIPS procedure is often guided by the clinical presentation of portal hypertension and its complications. In this cohort, the primary indication for TIPS was recurrent ascites, which was present in 36 patients (49%) across the study population. The breakdown of this indication by risk group was as follows: 13 patients (54%) in the low-risk group and 17 patients (53%) in the high-risk group. This suggests that recurrent ascites, a common complication of cirrhosis, was the most prevalent indication for TIPS in both risk groups, highlighting the significance of fluid accumulation and its clinical implications.

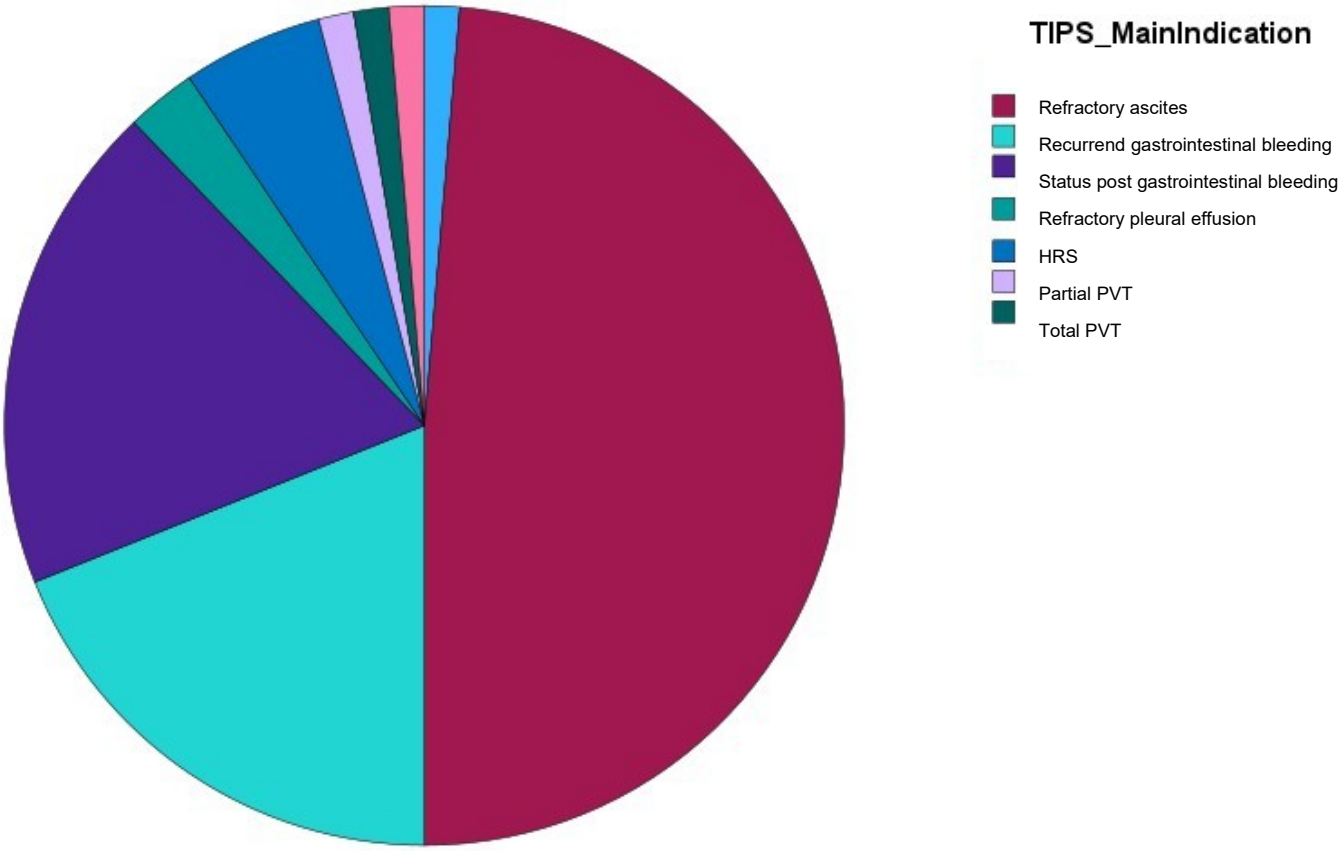

Figure 15: Distribution of TIPS Mainindication
Abbreveations: HRS, hepato-renal-syndrome; PVT, portal vein thrombosis

Additionally, recurrent gastrointestinal (GI) bleeding (more than two episodes) was the indication for TIPS in 14 patients (19%). 3 patients (13%) were in the low-risk group and 9 patients (28%) in the high-risk group.

Another significant indication for TIPS was active GI bleeding, which was as well seen in 14 patients (19%). Wherease 5 patients were in the low-risk group (21%) and also 5 in the high-risk group had (16%).

Finally, 9 patients (12%) underwent TIPS for other indications, such as severe portal hypertension that did not respond to medical therapy. These patients included 3 patients (13%) in the low-risk group and 1 patient (3%) in the high-risk group.

The CHILD-Pugh score is a widely used tool to assess liver function and the degree of liver cirrhosis. This score is a critical factor in predicting the prognosis and surgical outcomes in patients undergoing a TIPS procedure. The distribution of the CHILDPugh score in the overall cohort was as follows:

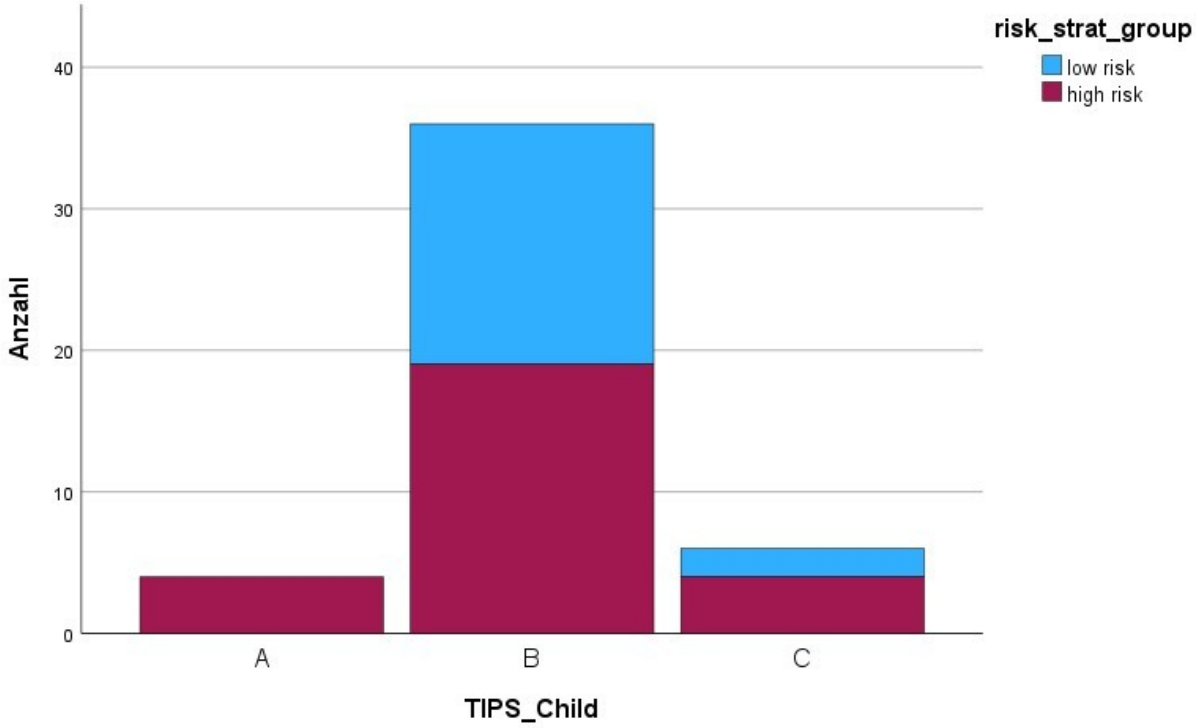

Figure 16: Distribution of Child Pugh Score within the risk groups

CHILD-Pugh A (compensated cirrhosis) was observed in 5 patients (7%). Notably, there were no patients in the low-risk group with a CHILD-Pugh A score (0%), but 4 patients (13%) in the high-risk group were classified as CHILD-Pugh A. This suggests that compensated cirrhosis, with preserved liver function, was relatively rare in this cohort, and when it occurred, it was slightly more common in the highrisk group.

CHILD-Pugh B (moderately decompensated cirrhosis) was the most common score, affecting 46 patients (62%). Of these, 17 patients (71%) were in the low-risk group, while 19 patients (59%) were in the high-risk group. This finding indicates that moderate liver dysfunction was predominant in the cohort, with a slightly higher proportion of low-risk patients having moderate cirrhosis. This is consistent with the expectation that moderate cirrhosis is often present in both high-risk and low-risk populations but may be associated with different outcomes.

CHILD-Pugh C (severely decompensated cirrhosis) was recorded in 8 patients (11%), with 2 patients (8%) in the low-risk group and 4 patients (13%) in the highrisk group. This relatively low proportion of patients with severe liver decompensation highlights the advanced stage of disease seen in these patients. The higher number of CHILD-Pugh C patients in the high-risk group further suggests that severe liver dysfunction, which is associated with a worse prognosis, is more prevalent in the high-risk cohort.

In summary, the distribution of etiology, indication for TIPS, and the CHILD-Pugh score in this cohort provides critical insights into the characteristics of patients undergoing TIPS. The majority of patients had alcohol-related liver disease, with a significant portion of patients in both risk groups requiring TIPS for recurrent ascites or GI bleeding. The CHILD-Pugh score revealed that most patients had moderate liver dysfunction (CHILD-Pugh B), with a smaller proportion suffering from severe liver decompensation (CHILD-Pugh C), particularly in the high-risk group. These findings underscore the complex interplay of liver disease severity, clinical indications, and risk stratification in the management of portal hypertension and its complications.

	Overall N=74						p-value
			Low risk (LAVI ≤ 34 mL/m², E/e' ≤ 10 and E/A ≤ 1.5) N=24		High risk (LAVI > 34 mL/m², E/e' > 10 or E/A > 1.5) N=32		
	Data available n (%)	Median [interquartile range]	Data available n (%)	Median [interquartile range]	Data available n (%)	Median [interquartile range]	
IVSed, mm	46 (62)	11.1[9.5-12]	17 (71)	9.7[9.2-11.2]	29 (91)	11.7[10.5-13.0]	0.080
PWed, mm	46 (62)	11.3[10-12.2]	17 (71)	10.5[9.3-11.8]	29 (91)	11.4[10.6-12.3]	0.148
LVEDD, mm	52 (70)	46.2[42.8-49.0]	17 (71)	47.0[43.0-48.7]	29 (91)	46.0[41.7-49.5]	0.838
LA diameter, mm	44 (60)	40.7[37.0-45.5]	17 (71)	38.5[35.7-40.4]	27 (84)	42.6[37.7-46.0]	**0.018**
LVEDV, mL	40 (54)	116.5[99.3-142.7]	15 (63)	123.1[91.4-135.8]	25 (78)	113.6[101.6-144.3]	0.706
LVESV, mL	40 (54)	51.1[42.5-72.1]	15 (63)	48.0[41.9-71.9]	25 (91)	52.4[43.1-72.4]	0.605
LVEF, %	40 (54)	54.0[48.8-59.5]	15 (63)	52.0[48.3-58.4]	25 (91)	54.3[49.4-60.0]	0.856
LVGLS, %	25 (34)	-21.3[-23.8-(-19,5)]	9 (38)	-20.7[-22.4-(-20.0)]	16 (84)	-21.4[-24.4-(-19.2)]	0.821
LASr, %	35 (47)	41.5[27.8-46.8]	12 (50)	46.4[38.6-48.3]	23 (91)	32.5[25.5-45.2]	**0.031**
RVEDD basal, mm	39 (53)	36.2[29.5-39.5]	12 (50)	35.8[29.3-40.8]	27 (91)	36.4[29.9-38.7]	0.903
RVFAC, %	37 (50)	44.7[40.6-49.4]	12 (50)	46.5[35.2-54]	25 (84)	44.1[41.0-48.0]	0.381
RVFWS, %	31 (42)	-26.5[-31.4-(-22.3)]	11 (46)	-26.6[-29.8-(-22.3)]	20 (84)	-25.4[-31.9-(-22.4)]	0.650
RVLS, %	31 (42)	-23.5[-27.4-(-20.2)]	11 (46)	-24.0[-27.4-(-19.7)]	20 (78)	-21.7[-28.3-(-20.5)]	0.606
E, m/s	55 (74)	0.81[0.71-0.98]	24 (100)	0.78[0.62-0.84]	31 (91)	0.90[0.74-1.09]	**0.005**
A, m/s	55 (74)	0.76[0.61-0.92]	24 (100)	0.78[0.70-0.92]	31 (94)	0.75[0.56-1.05]	0.513
E/A	54 (73)	1.08[0.86-1.50]	24 (100)	0.93[0.80-1.11]	30 (78)	1.42[0.90-1.64]	**0.002**
TAPSE, mm	33 (45)	25.7[23.7-29.2]	13 (54)	25.0[24.5-27.7]	20 (75)	26.8[23.1-29.5]	0.484
TRVmax, m/s	40 (54)	2.38[2.01-2.67]	14 (58)	1.98[1.61-2.18]	26 (72)	2.60[2.34-2.78]	**< 0.001**
VCI diameter, mm	8 (11)	16.4[13.7-20.9]	2 (8)	17.1[12.9-21.3]	6 (72)	16.4[14.5-20.5]	1.000
LAVI, mL/m²	27 (37)	33.3[27.1-39.04]	11 (46)	27.1[20.8-31.4]	16 (78)	38.5[34.4-40.2]	**< 0.001**
E/e'	46 (62)	9.50[8.45-12.70]	17 (71)	8.76[8.27-9.47]	29 (91)	12.13[9.00-14.50]	**0.001**

Table 3: Echocardiographic parameters, overall and stratified by risk

Abbreveations: IVSed, end-diastolic interventricular septum thickness; PWed, enddiastolic posterior wall thickness; LVEDD, left ventricular end-diastolic diameter; LA, left atrium; LVEDV, left ventricular end-diastolic volume, LVESV, left ventricular end-systolic volume; LVEF, left ventricular ejection fraction; LVGLS, left ventricular global longitudinal strain; LASr, left atrial reservoir strain; RVEDD basal, basal right ventricular end-diastolic diameter; RVFAC, right ventricular fractional area change; RVFWS, right ventricular free wall strain; RVLS, right ventricular longitudinal strain; TAPSE, tricuspid annular plane systolic excursion; TRVmax, maximum tricuspid regurgitant velocity; VCI, vena cava inferior; LAVI; left atrial volume index.

3.2. Echocardiographic Parameters

Tricuspid Regurgitation Velocity (TRVmax): A notable difference between the groups was observed in the maximum tricuspid regurgitation velocity. In the low-risk group, the TRVmax was significantly lower (1.98 m/s) than in the high-risk group (2.60 m/s), with this difference being highly significant ($p < 0.001$).

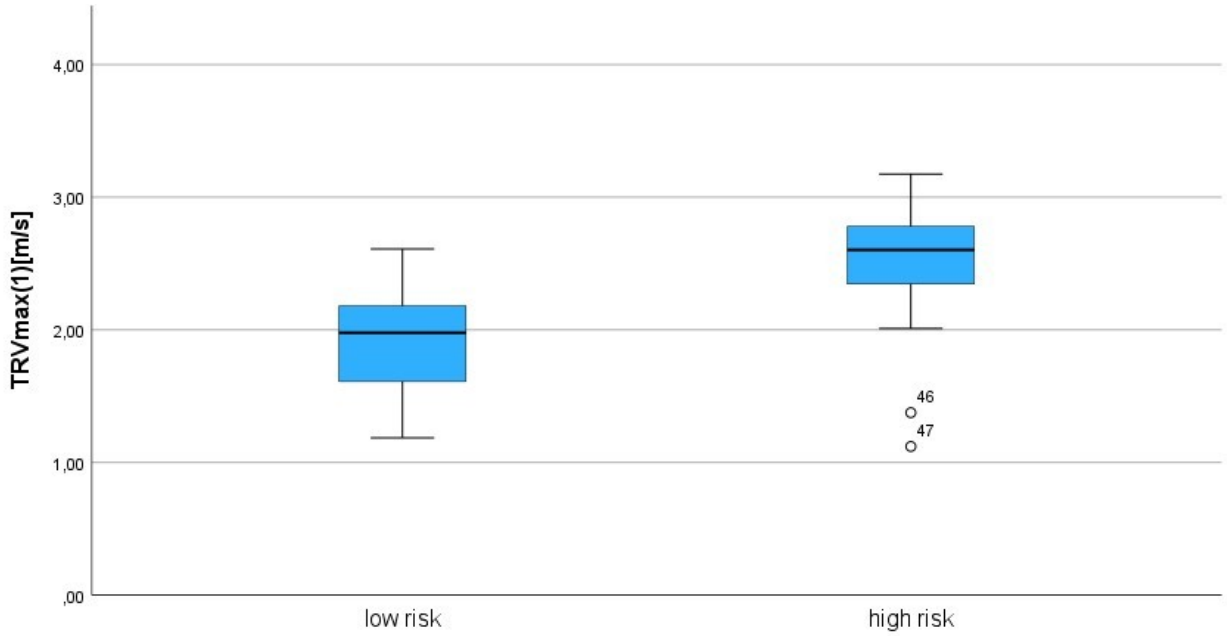

Figure 17: Boxplot of TRVmax Distribution within the risk groups
Abbreveations: TRVmax, maximum of tricuspid valve regurgitation velocity

Left Atrial Volume Index (LAVI): The median LAVI for the overall group was 33.3 mL/m² (IQR: 27.1-39.04 mL/m²). In the low-risk group, the LAVI was lower (27.1 mL/m², IQR: 20.8-31.4 mL/m²) compared to the high-risk group (38.5 mL/m², IQR: 34.4-40.2 mL/m²), and this difference was statistically significant ($p < 0.001$).

The E/e' ratio, a measure of diastolic function, was significantly lower in the low-risk group (8.76, IQR: 8.27-9.47) compared to the high-risk group (12.13, IQR: 9.00-14.50), with a highly significant difference ($p = 0.001$).

Furthermore, the LA reservoir strain and the LA Diameter have also been significantly different between the low and the high-risk group. The LA reservoir strain in the low-risk group was 46.40% [38.6-48.3], while in the high-risk it showed values of 32.5% [25.5-45.2]. The LA Diameter was dilated with 42.6mm [37.7-46.0] in the high-risk group, while it was still in a normal range with 38.5mm [35.7-40.4] in the low-risk group.

In summary the values presented in the table confirm the differences in cardiac function between the low- and high-risk groups. Patients in the low-risk group exhibited significantly better results in terms of tricuspid regurgitation, left atrial reservoir strain und had no dilation of the left atrium, indicating less impaired cardiovascular function. Notably, the LAVI and E/e' values showed the most substantial differences between the groups, reflecting significant variations in left ventricular diastolic function. These differences effectively illustrate the utility of echocardiographic parameters in risk stratification and provide insight into the underlying cardiovascular status of patients in these two risk categories.

4. Discussion

There were no statistically significant differences observed between the groups with regard to systolic cardiac parameters or right ventricular function. These findings suggest that, at least from a systolic standpoint, the two groups exhibited similar cardiac performance at rest. This includes parameters typically used to assess the systolic function, such as LVEF or LVGLS and of the right heart performance, such as TAPSE or RVFAC. All of these parameters showed no significant difference between the groups, suggesting that the systolic function is similar.

However, the parameters related to diastolic function revealed marked and statistically significant differences. Patients classified as belonging to the high-risk group demonstrated considerably elevated values in LA diameter, E/e′ ratio, E/A artio, left atrial volume index (LAVI) and decreased values in the LA strain. Moreover, the high-risk group also exhibited significantly higher TRVmax indicating

higher pulmonary artery pressures as possible signs of left ventricular dysfunction. However, in the high-risk group the majority of patients had estimated normal pulmonary artery pressures.

Taken together, these findings underscore the prognostic relevance of diastolic function parameters in patients being considered for a TIPS implantation. Diastolic markers appear to offer valuable insights into underlying cardiovascular risk and the patient's capacity to tolerate hemodynamic shifts induced by the shunt procedure.

It is hypothesized that in many of these high-risk patients, a form of cirrhotic and / or alcohol-related cardiomyopathy may already be present prior to the TIPS procedure. Such underlying cardiomyopathies could be the reason for a compromised ability of the heart to adapt to stress or volume changes, even when systolic function appears preserved. When the TIPS is placed, it introduces a significant hemodynamic volume shift, increasing venous return and cardiac preload. In patients with pre-existing myocardial impairment - particularly involving diastolic dysfunction - this additional load may exceed the compensatory capacity of the heart, potentially leading to cardiac decompensation. This mechanism could explain the high number of cardiac decompensations after a TIPS implantation.

In order to further validate the Toulouse Algorithm, it will be crucial to analyze the collect data of cardiac decompensation events occurring within the first year following TIPS implantation.

The study “the Toulouse algorithm identifies patients with increased risk of cardiac decompensation only in patients with TIPS for refractory ascites” by Vanderschueren et al. (2025) addresses an important clinical concern: the risk of cardiac decompensation (CD) following TIPS placement. This retrospective analysis contributes meaningfully by evaluating the predictive value of the Toulouse algorithm, particularly in patients with refractory ascites. The authors present a clear correlation between certain baseline markers and the development of CD, but notably only within the ascites subgroup. This distinction underscores the heterogeneity of the TIPS population—something often overlooked in broader

studies. Importantly, while the Toulouse algorithm showed predictive value in one subgroup, its failure to perform similarly in patients with variceal bleeding raises questions about its broader clinical utility. Nonetheless, the study highlights the need for more tailored risk stratification tools and advocates for close post-TIPS monitoring in high-risk patients rather than withholding treatment. [47]

In summary, the Toulouse algorithm appears to be a useful tool for identifying cardiac risk in patients undergoing TIPS for refractory ascites, but it does not demonstrate the same predictive value in those treated for esophageal variceal bleeding.

When comparing the findings of this study with those of previous research evaluating the Toulouse algorithm, notable similarities become apparent. In the present study, patients generally showed normal left ventricular ejection fraction (LVEF), normal global longitudinal strain (GLS), and only minimal variations in diastolic function parameters. These echocardiographic findings are consistent with those reported in the study by Vanderschueren et al. or the study of Venner M. et al., which also observed largely normal cardiac function at baseline in their patient cohort. [47], [48] Moreover, additional comprehensive analyses will be necessary to better understand the predictive value of various echocardiographic and clinical parameters. Such investigations would provide a more robust foundation for risk stratification and ultimately contribute to the development of improved patient selection criteria and peri-procedural management strategies.

4.1 Limitations

However, it is also important to acknowledge several key limitations of our study, which must be taken into account when interpreting the findings. First and foremost, the overall sample size was relatively small, comprising only 74 patients in total and only 56 patients in the risk groups. While our results do offer important preliminary insights, the limited cohort size inevitably restricts the generalizability of our conclusions to broader clinical populations. Larger, multicenter studies will be

necessary to confirm our observations and ensure that they are applicable across diverse patient groups and clinical settings.

In addition, the quality of the echocardiographic data available to us was not optimal in all cases. As echocardiography is a highly operator-dependent imaging modality, variability in image acquisition and interpretation may have influenced the precision of the measurements. There was also not an equal quality guaranteed in the echocardiograms of 2004 compared with the ones from 2024. Due to this limitations the analysis of all echocardiographic parameters was not possible in many patients.

Another notable limitation is the absence of NT-proBNP data for our patient cohort. This biomarker, which reflects myocardial wall stress and is frequently elevated in heart failure, constitutes a central component of the Toulouse Algorithm. Due to the lack of NT-proBNP measurements in our dataset, we were only able to conduct a partial validation of the Toulouse Algorithm. This limitation reduces the completeness and strength of our algorithm-based risk assessment and underscores the need for future studies to incorporate comprehensive biomarker profiling, including natriuretic peptides, in order to validate and potentially refine existing prognostic models.

Finally, it must be emphasized that the systematic collection of data on postprocedural cardiac decompensation events in our patient population is still ongoing. As a result, we are currently unable to provide definitive conclusions regarding the incidence and timing of such events within the first year following TIPS implantation. This information will be essential for evaluating the true prognostic value of preprocedural echocardiographic and clinical parameters. The completion of this followup and the incorporation of these data into future analyses will be done in the near future.

4.2 Strengths

The strengths of this study lie primarily in the highly detailed analysis of the transthoracic echocardiograms. In total, 48 different echocardiographic parameters were evaluated, allowing for a comprehensive assessment of cardiac function. A particularly important aspect to emphasize is that all measurements were performed manually by myselve, ensuring consistency and quality control. Furthermore, each parameter was measured twice- during two separate cardiac cycles- and the median value was used in our analysis. This approach was chosen deliberately to reduce variability and minimize potential measurement errors.

Another major strength of this study is the extensive clinical registry it is build on. This registry provided rich and detailed information not only about the TIPS procedure itself but also about the patients' clinical status both before and after the intervention. This complete and thorough data on all patient characteristics-, enabled a more precise and context-aware interpretation of the echocardiographic findings and their clinical implications.

4.3 Conclusion

Despite these limitations, the findings of this thesis clearly indicate that echocardiographic parameters play a crucial role in the pre-interventional risk assessment of patients undergoing a TIPS Implantation. The identification of significant associations between diastolic dysfunction markers and patient risk underscores the potential of echocardiography as a valuable, non-invasive diagnostic tool in the preoperative assessment. A thorough cardiovascular workup, including comprehensive echocardiography and, where feasible, biomarker analysis, would allow for the early detection of pre-existing cardiac impairment. Recognizing such vulnerabilities in advance is essential for appropriately stratifying patients based on risk, tailoring perioperative management strategies, and ultimately minimizing the likelihood of post-procedural cardiac complications.

To build upon these insights and strengthen the evidence base, further prospective studies are needed. Such investigations should aim to validate our observations in

larger and more diverse patient populations, incorporate standardized cardiac biomarker profiles such as NT-proBNP, and include long-term follow-up data on cardiac events after TIPS placement. Continued research in this area holds significant promise for enhancing the safety and efficacy of TIPS procedures, particularly in patients with underlying cardiac dysfunction.

5. Bibliography

[1] Y.-B. Liu and M.-K. Chen, ‘Epidemiology of liver cirrhosis and associated complications: Current knowledge and future directions’, *World J Gastroenterol*, vol. 28, no. 41, pp. 5910–5930, Nov. 2022, doi: 10.3748/wjg.v28.i41.5910.

[2] L. Pimpin *et al.*, ‘Burden of liver disease in Europe: Epidemiology and analysis of risk factors to identify prevention policies’, *J Hepatol*, vol. 69, no. 3, pp. 718–735, Sep. 2018, doi: 10.1016/j.jhep.2018.05.011.

[3] Ĺ. Skladaný *et al.*, ‘Hepatic venous pressure gradient in patients with (compensated and decompensated) advanced chronic liver disease – A comparison of metabolic dysfunction-associated steatotic liver disease with alcohol-associated liver disease: A retrospective view’, *PLoS One*, vol. 20, no. 3, p. e0317287, Mar. 2025, doi: 10.1371/journal.pone.0317287.

[4] M. Blachier, H. Leleu, M. Peck-Radosavljevic, D.-C. Valla, and F. RoudotThoraval, ‘The burden of liver disease in Europe: A review of available epidemiological data’, *J Hepatol*, vol. 58, no. 3, pp. 593–608, Mar. 2013, doi: 10.1016/j.jhep.2012.12.005.

[5] W. A. Zatoński *et al.*, ‘Liver Cirrhosis Mortality in Europe, with Special Attention to Central and Eastern Europe’, *Eur Addict Res*, vol. 16, no. 4, pp. 193–201, 2010, doi: 10.1159/000317248.

[6] V. Sivanathan *et al.*, ‘Ätiologie und Komplikationen der Leberzirrhose: Daten eines deutschen Zentrums’, *DMW - Deutsche Medizinische Wochenschrift*, vol. 139, no. 36, pp. 1758–1762, Aug. 2014, doi: 10.1055/s-0034-1387240.

[7] T. Vos *et al.*, ‘Global burden of 369 diseases and injuries in 204 countries and territories, 1990–2019: a systematic analysis for the Global Burden of Disease Study 2019’, *The Lancet*, vol. 396, no. 10258, pp. 1204–1222, Oct. 2020, doi: 10.1016/S0140-6736(20)30925-9.

[8] D. A. Brenner, ‘Reversibility of liver fibrosis.’, *Gastroenterol Hepatol (N Y)*, vol. 9, no. 11, pp. 737–9, Nov. 2013.

[9] I. R. Wanless, E. Nakashima, and M. Sherman, ‘Regression of Human Cirrhosis’, *Arch Pathol Lab Med*, vol. 124, no. 11, pp. 1599–1607, Nov. 2000, doi: 10.5858/2000-124-1599-ROHC.

[10] A. Baiges and J. C. Garcia-Pagán, ‘Predicting Heart Failure After TIPS: Still More Questions Than Answers’, *Hepatology*, vol. 70, no. 6, pp. 1889–1891, Dec. 2019, doi: 10.1002/hep.30948.

[11] H. Schneider *et al.*, ‘Diastolic dysfunction is associated with cardiac decompensation after transjugular intrahepatic portosystemic shunt in patients with liver cirrhosis’, *United European Gastroenterol J*, vol. 11, no. 9, pp. 837–851, Nov. 2023, doi: 10.1002/ueg2.12471.

[12] G. D’Amico, G. Garcia-Tsao, and L. Pagliaro, ‘Natural history and prognostic indicators of survival in cirrhosis: A systematic review of 118 studies’, *J Hepatol*, vol. 44, no. 1, pp. 217–231, Jan. 2006, doi: 10.1016/j.jhep.2005.10.013.

[13] C. Billey *et al.*, ‘A Prospective Study Identifying Predictive Factors of Cardiac Decompensation After Transjugular Intrahepatic Portosystemic Shunt: The Toulouse Algorithm’, *Hepatology*, vol. 70, no. 6, pp. 1928–1941, Dec. 2019, doi: 10.1002/hep.30934.

[14] H. Strunk and M. Marinova, ‘Transjugular Intrahepatic Portosystemic Shunt (TIPS): Pathophysiologic Basics, Actual Indications and Results with Review of the Literature’, *RöFo - Fortschritte auf dem Gebiet der Röntgenstrahlen und der bildgebenden Verfahren*, vol. 190, no. 08, pp. 701–711, Aug. 2018, doi: 10.1055/a-0628-7347.

[15] O. Yumusak, ‘Update on cirrhotic cardiomyopathy: from etiopathogenesis to treatment’, *Ann Gastroenterol*, 2024, doi: 10.20524/aog.2024.0885.

[16] S. Møller and J. H. Henriksen, ‘Cirrhotic cardiomyopathy’, *J Hepatol*, vol. 53, no. 1, pp. 179–190, Jul. 2010, doi: 10.1016/j.jhep.2010.02.023.

[17] S. K. Baik, T. R. Fouad, and S. S. Lee, ‘Cirrhotic cardiomyopathy.’, *Orphanet J Rare Dis*, vol. 2, p. 15, Mar. 2007, doi: 10.1186/1750-1172-2-15.

[18] S. Møller and J. H. Henriksen, ‘Cardiovascular Dysfunction in Cirrhosis: Pathophysiological Evidence of a Cirrhotic Cardiomyopathy’, *Scand J Gastroenterol*, vol. 36, no. 8, pp. 785–794, Aug. 2001, doi: 10.1080/003655201750313289.

[19] E. Tanai and S. Frantz, ‘Pathophysiology of Heart Failure’, in *Comprehensive Physiology*, Wiley, 2015, pp. 187–214. doi: 10.1002/cphy.c140055.

[20] M. Di Pascoli, D. Sacerdoti, P. Pontisso, P. Angeli, and M. Bolognesi, ‘Molecular Mechanisms Leading to Splanchnic Vasodilation in Liver Cirrhosis’, *J Vasc Res*, vol. 54, no. 2, pp. 92–99, 2017, doi: 10.1159/000462974.

[21] E. Seki and R. F. Schwabe, ‘Hepatic inflammation and fibrosis: Functional links and key pathways’, *Hepatology*, vol. 61, no. 3, pp. 1066–1079, Mar. 2015, doi: 10.1002/hep.27332.

[22] R. M. Lang *et al.*, ‘Recommendations for Cardiac Chamber Quantification by Echocardiography in Adults: An Update from the American Society of Echocardiography and the European Association of Cardiovascular Imaging’, *Journal of the American Society of Echocardiography*, vol. 28, no. 1, pp. 1-39.e14, Jan. 2015, doi: 10.1016/j.echo.2014.10.003.

[23] S. F. Nagueh *et al.*, ‘Recommendations for the Evaluation of Left Ventricular Diastolic Function by Echocardiography: An Update from the American Society of Echocardiography and the European Association of Cardiovascular Imaging’, *Eur Heart J Cardiovasc Imaging*, vol. 17, no. 12, pp. 1321–1360, Dec. 2016, doi: 10.1093/ehjci/jew082.

[24] M. Izzy *et al.*, ‘Redefining Cirrhotic Cardiomyopathy for the Modern Era’, *Hepatology*, vol. 71, no. 1, pp. 334–345, Jan. 2020, doi: 10.1002/hep.30875.

[25] B. P. Halliday, R. Senior, and D. J. Pennell, ‘Assessing left ventricular systolic function: from ejection fraction to strain analysis’, *Eur Heart J*, vol. 42, no. 7, pp. 789–797, Feb. 2021, doi: 10.1093/eurheartj/ehaa587.

[26] C. Andersson, M. Schou, F. Gustafsson, and C. Torp-Pedersen, ‘Alcohol Intake in Patients With Cardiomyopathy and Heart Failure: Consensus and Controversy’, *Circ Heart Fail*, vol. 15, no. 8, Aug. 2022, doi: 10.1161/CIRCHEARTFAILURE.121.009459.

[27] M. G. Griswold *et al.*, ‘Alcohol use and burden for 195 countries and territories, 1990–2016: a systematic analysis for the Global Burden of Disease Study 2016’, *The Lancet*, vol. 392, no. 10152, pp. 1015–1035, Sep. 2018, doi: 10.1016/S0140-6736(18)31310-2.

[28] R. Hingson, W. Zha, and D. Smyth, ‘Magnitude and Trends in Heavy Episodic Drinking, Alcohol-Impaired Driving, and Alcohol-Related Mortality and

Overdose Hospitalizations Among Emerging Adults of College Ages 18–24 in the United States, 1998–2014', *J Stud Alcohol Drugs*, vol. 78, no. 4, pp. 540–548, Jul. 2017, doi: 10.15288/jsad.2017.78.540.

[29] F. Domínguez, E. Adler, and P. García-Pavía, 'Alcoholic cardiomyopathy: an update', *Eur Heart J*, vol. 45, no. 26, pp. 2294–2305, Jul. 2024, doi: 10.1093/eurheartj/ehae362.

[30] Y. Liang *et al.*, 'Chronic Alcohol Intake Exacerbates Cardiac Dysfunction After Myocardial Infarction', *Alcohol and Alcoholism*, vol. 55, no. 5, pp. 524–530, Aug. 2020, doi: 10.1093/alcalc/agaa055.

[31] P. Vaideeswar, C. Chaudhari, S. Rane, J. Gondhalekar, and S. Dandekar, 'Cardiac pathology in chronic alcoholics', *J Postgrad Med*, vol. 60, no. 4, pp. 372–376, 2014, doi: 10.4103/0022-3859.143958.

[32] Y. Wang, G. Li, Y. Sun, G. Shan, R. Xu, and L. Guo, 'Left Ventricular Strain and Rotation by 2-D Speckle Tracking Echocardiography Identify Early Alcoholic Cardiomyopathy', *Ultrasound Med Biol*, vol. 42, no. 8, pp. 1741–1749, Aug. 2016, doi: 10.1016/j.ultrasmedbio.2016.03.023.

[33] A. Askanas, M. Udoshi, and S. A. Sadjadi, 'The heart in chronic alcoholism: a noninvasive study', *Am Heart J*, vol. 99, no. 1, pp. 9–16, Jan. 1980, doi: 10.1016/0002-8703(80)90309-9.

[34] A. Askanas, M. Udoshi, and S. A. Sadjadi, 'The heart in chronic alcoholism: a noninvasive study', *Am Heart J*, vol. 99, no. 1, pp. 9–16, Jan. 1980, doi: 10.1016/0002-8703(80)90309-9.

[35] P. Rodrigues *et al.*, 'Association Between Alcohol Intake and Cardiac Remodeling', *J Am Coll Cardiol*, vol. 72, no. 13, pp. 1452–1462, Sep. 2018, doi: 10.1016/j.jacc.2018.07.050.

[36] A. M. Lazarević *et al.*, 'Early changes in left ventricular function in chronic asymptomatic alcoholics: relation to the duration of heavy drinking', *J Am Coll Cardiol*, vol. 35, no. 6, pp. 1599–1606, May 2000, doi: 10.1016/S07351097(00)00565-9.

[37] M. Kucuk, C. R. Oncel, A. Belgi Yıldırım, F. Canan, and M. M. Kuloglu, 'Evaluation of Subclinical Left Ventricular Systolic Dysfunction in Chronic

Asymptomatic Alcoholics by Speckle Tracking Echocardiography', *Biomed Res Int*, vol. 2017, pp. 1–6, 2017, doi: 10.1155/2017/6582568.

[38] S. Omerovic and A. Jain, *Echocardiogram*. 2025.

[39] N. Bom, A. F. W. Van Der Steen, N. De Jong, and J. R. T. C. Roelandt, 'Early, recent and future applications of echocardiography*', *Clin Physiol Funct Imaging*, vol. 24, no. 3, pp. 141–146, May 2004, doi: 10.1111/j.1475097X.2004.00541.x.

[40] G. S. Mintz, M. N. Kotler, W. R. Parry, and B. L. Segal, 'Statistical comparison of M mode and two dimensional echocardiographic diagnosis of flail mitral leaflets', *Am J Cardiol*, vol. 45, no. 2, pp. 253–259, Feb. 1980, doi: 10.1016/0002-9149(80)90643-8.

[41] I. Edler and C. H. Hertz, 'The Use of Ultrasonic Reflectoscope for the Continuous Recording of the Movements of Heart Walls.', *Clin Physiol Funct Imaging*, vol. 24, no. 3, pp. 118–136, May 2004, doi: 10.1111/j.1475097X.2004.00539.x.

[42] N. Bom, A. F. W. Van Der Steen, N. De Jong, and J. R. T. C. Roelandt, 'Early, recent and future applications of echocardiography*', *Clin Physiol Funct Imaging*, vol. 24, no. 3, pp. 141–146, May 2004, doi: 10.1111/j.1475097X.2004.00541.x.

[43] X. LI *et al.*, 'A novel method for the assessment of the accuracy of computing laminar flow stroke volumes using a real-time 3D ultrasound system: In vitro studies', *European Journal of Echocardiography*, vol. 6, no. 6, pp. 396–404, Dec. 2005, doi: 10.1016/j.euje.2005.04.010.

[44] I. M. Coman and B. A. Popescu, 'Shigeo Satomura: 60 years of Doppler ultrasound in medicine', *Cardiovasc Ultrasound*, vol. 13, no. 1, p. 48, Dec. 2015, doi: 10.1186/s12947-015-0042-3.

[45] I. Ahmed and N. Sasikumar, *Echocardiography Imaging Techniques*. 2025.

[46] C. R. Tainter and S. Nhieu, 'Point-of-Care Transthoracic Echocardiography: Probe Manipulation, Positioning, and Essential Views', in *Essential Echocardiography*, Cham: Springer International Publishing, 2022, pp. 47–60. doi: 10.1007/978-3-030-84349-6_3.

[47] E. Vanderschueren *et al.*, ‘The Toulouse algorithm identifies patients with increased risk of cardiac decompensation only in patients with TIPS for refractory ascites’, *Ann Hepatol*, vol. 30, no. 1, p. 101568, Jan. 2025, doi: 10.1016/j.aohep.2024.101568.

[48] M. F. G. H. M. Venner *et al.*, ‘Diastolic dysfunction as predictive parameter for the development of post-TIPS cardiac decompensation’, *Int J Cardiol*, vol. 431, p. 133226, Jul. 2025, doi: 10.1016/j.ijcard.2025.133226.

6. Appendix

echo parameters	entire cohort n=74					risk stratification group									
						low risk n=24					high risk n=32				
	absolute frequency	relative frequency [%]	median	percentile 25	percentile 75	absolute frequency	relative frequency [%]	median	percentile 25	percentile 75	absolute frequency	relative frequency [%]	median	percentile 25	percentile 75
IVSed_PLAX [mm]	46	62,16%	11,13	9,47	12,95	17	70,83%	9,74	9,19	11,20	29	90,63%	11,67	10,47	12,95
PWed_PLAX [mm]	46	62,16%	11,33	9,91	12,22	17	70,83%	10,05	9,25	11,78	29	90,63%	11,43	10,58	12,26
LVEDD_PLAX [mm]	52	70,27	46,2	42,8	49,0	17	70,83%	47,0	43,0	48,7	29	90,63%	46,0	41,7	49,5
LAdiameter_PLAX [mm]	44	59,46%	40,55	36,94	45,53	17	70,83%	38,49	35,68	40,39	27	84,38%	42,58	37,67	45,96
LVEDV_a4c [cm³]	46	62,16%	118,64	96,77	143,75	19	79,17%	117,67	92,87	128,97	27	84,38%	129,10	99,66	161,69
LVESV_a4c [cm³]	46	62,16%	48,62	44,58	69,83	19	79,17%	49,25	43,46	61,64	27	84,38%	54,04	44,68	75,19
LVEDV_a2c [cm³]	42	56,76%	116,52	89,80	139,09	15	62,50%	107,47	81,38	130,98	27	84,38%	119,75	93,46	149,04
LVESV_a2c [cm³]	42	56,76%	47,87	38,21	68,41	15	62,50%	43,26	38,17	63,63	27	84,38%	54,47	38,56	68,79
LVEDV_biplane [cm³]	40	54,05%	116,04	99,25	142,65	15	62,50%	123,09	91,43	135,77	25	78,13%	113,62	101,56	144,25
LVESV_biplane [cm³]	40	54,05%	51,10	42,52	72,13	15	62,50%	47,95	41,91	71,93	25	78,13%	52,41	43,07	72,35
LVEF_biplane [%]	40	54,05%	54,00	48,83	59,53	15	62,50%	52,00	48,25	58,35	25	78,13%	54,25	49,40	60,00
LVGLS_autostrain [%]	25	33,78%	-21,30	-23,80	-19,45	9	37,50%	-20,70	-22,40	-19,95	16	50,00%	-21,42	-24,35	-19,23
IVSed_a4c [mm]	49	66,22%	10,61	9,19	11,92	20	83,33%	9,18	8,32	10,92	29	90,63%	11,16	9,64	12,17
PWed_a4c [mm]	49	66,22%	10,55	9,63	11,65	20	83,33%	9,84	9,06	11,16	29	90,63%	10,99	10,23	11,69
LVEDD_a4c [mm]	49	66,22%	44,31	38,65	51,63	20	83,33%	43,58	39,82	48,93	29	90,63%	44,67	37,76	51,65
LAarea_ES_a4c [cm²]	51	68,92%	20,27	16,98	23,56	21	87,50%	17,38	15,81	20,53	30	93,75%	21,70	19,35	24,22
LAarea_ES_a2c [cm²]	39	52,70%	20,40	16,74	23,91	14	58,33%	18,20	16,15	20,97	25	78,13%	20,61	18,46	23,91
LAlength_ES_a4c [mm]	53	71,62%	52,90	48,07	56,71	23	95,83%	50,11	44,99	55,70	30	93,75%	54,50	51,66	59,40
LAlength_ES_a2c [mm]	39	52,70%	54,83	49,93	58,51	14	58,33%	51,69	49,91	54,83	25	78,13%	55,65	51,24	59,40
LAV_ES_biplane [cm³]	38	51,35%	61,87	49,52	74,57	14	58,33%	51,74	43,00	57,92	24	75,00%	68,20	60,05	78,57
LASr_ED [%]	35	47,30%	41,50	27,80	46,75	12	50,00%	46,35	38,55	48,33	23	71,88%	32,50	25,50	45,15
LASct_ED [%]	35	47,30%	-23,65	-28,65	-16,30	12	50,00%	-27,17	-29,45	-18,95	23	71,88%	-20,40	-27,80	-13,90

Table 4: Appendix: all echocardiographic parameters, overall and stratified by risk I

Abbreviations: IVSed, end-diastolic interventricular septum thickness; PWed, end-diastolic posterior wall thickness; LVEDD, left ventricular end-diastolic diameter; LA, left atrium; LA_dia, left atrial diameter; LVEDV, left ventricular end-diastolic volume, LVESV, left ventricular end-systolic volume; LVEF, left ventricular ejection fraction; LVGLS, left ventricular global longitudinal strain; LASr, left atrial reservoir strain

LASct_ED [%]	35	47,30%	-16,90	-20,60	-11,00	12	50,00%	-18,65	-22,75	-17,10	23	71,88%	-13,35	-18,65	-9,60
RVEDDbasal [mm]	39	52,70%	36,16	29,50	39,49	12	50,00%	35,83	29,32	40,78	27	84,38%	36,38	29,90	38,67
RVEDD_mid [mm]	37	50,00%	25,12	21,27	30,28	12	50,00%	28,00	20,48	33,47	25	78,13%	24,58	21,42	28,00
RVEDL [mm]	37	50,00%	73,22	70,00	78,05	12	50,00%	73,11	69,19	81,82	25	78,13%	75,16	70,00	77,48
RVAd [cm²]	37	50,00%	18,69	15,01	21,07	12	50,00%	19,47	15,73	21,92	25	78,13%	18,69	14,66	21,07
RVAs [cm²]	37	50,00%	10,74	7,71	12,21	12	50,00%	11,08	8,27	12,62	25	78,13%	10,70	7,71	12,21
RVFAC [%]	37	50,00%	44,65	40,55	49,35	12	50,00%	46,50	35,22	54,00	25	78,13%	44,05	40,95	47,95
RVFWSL [%]	31	41,89%	-26,45	-31,40	-22,30	11	45,83%	-26,60	-29,80	-22,30	20	62,50%	-25,40	-31,90	-22,35
RV4CSL [%]	31	41,89%	-23,50	-27,40	-20,20	11	45,83%	-24,00	-27,40	-19,70	20	62,50%	-21,65	-28,25	-20,48
RAarea_ES [cm²]	45	60,81%	14,98	13,06	17,76	18	75,00%	14,08	12,63	16,29	27	84,38%	15,05	13,10	17,80
RAlength_ES [mm]	49	66,22%	51,25	47,28	59,45	20	83,33%	48,73	46,37	54,64	29	90,63%	54,87	50,05	60,00
RAV_ES [cm³]	45	60,81%	35,53	28,45	45,07	18	75,00%	32,69	28,45	40,12	27	84,38%	37,38	27,43	45,48
eprime_medial [m/s]	47	63,51%	0,09	0,06	0,10	17	70,83%	0,09	0,08	0,09	30	93,75%	0,08	0,06	0,11
eprime_lateral [m/s]	22	29,73%	0,10	0,08	,013	10	41,67%	0,10	0,09	0,13	12	37,50%	0,10	0,07	0,13
Ewave [m/s]	55	74,32%	0,81	0,71	0,98	24	100%	0,73	0,62	0,84	31	96,88%	0,90	0,74	1,09
Awave [m/s]	55	74,32%	0,76	0,61	0,92	24	100%	0,78	0,70	0,92	31	96,88%	0,75	0,56	1,05
E/e' med	46	62,16%	9,50	8,45	12,70	17	70,83%	8,76	8,27	9,47	29	90,63%	12,13	9,00	14,50
E/e' lat	22	29,73%	7,63	6,55	8,82	10	41,67%	7,08	5,82	7,63	12	37,50%	8,78	7,46	13,32
E/A	54	72,98%	1,08	0,86	1,50	24	100%	0,93	0,80	1,11	30	93,75%	1,42	0,90	1,64
TAPSE [mm]	33	44,59%	25,71	23,68	29,22	13	54,17%	25,04	24,45	27,65	20	62,50%	26,84	23,14	29,53
sprime_lateral [m/s]	5	6,76%	0,15	0,15	0,16	0	0,0%				5	15,63%	0,15	0,15	0,16
TRVmax [m/s]	40	54,05%	2,38	2,01	2,67	14	58,33%	1,98	1,61	2,18	26	81,25%	2,60	2,34	2,78
VCIdiameter [mm]	8	10,81%	16,38	13,70	20,92	2	8,33%	17,12	12,94	21,31	6	18,75%	16,38	14,45	20,54
BSA [m²]	34	45,95%	1,90	1,71	1,99	13	54,17%	1,83	1,59	1,96	21	65,63%	1,95	1,72	1,99
LAVI_biplane [mL/m²]	27	36,49%	33,32	27,12	39,04	11	45,83%	27,12	20,80	31,42	16	50,00%	38,50	34,35	40,22
RAVI [mL/m²]	31	41,89%	19,24	14,69	21,75	12	50,00%	18,45	16,25	20,41	19	59,38%	20,83	13,39	22,03

Table 5: Appendix: all echocardiographic parameters, overall and stratified by risk II

RVEDD_basal/mid, basal/mid right ventricular end-diastolic diameter; RVFAC, right ventricular fractional area change; RVFWSL, right ventricular free wall strain; RV4CLS, right ventricular longitudinal strain; RAV, right ventricular volume; TAPSE, tricuspid annular plane systolic excursion; TRVmax, maximum tricuspid regurgitant velocity; VCI, vena cava inferior; BSA, body surface area; LAVI; left atrial volume index; RAVI, right atrial volume index

Patient's Characteristics														
	absolute frequency	relative frequency [%]	median	percentile 25	percentile 75	absolute frequency	relative frequency [%]	median	percentile 25	percentile 75	absolute frequency	relative frequency [%]	median	percentile 25	percentile 75
AGE	**74**	100%	**60**	53	67	**24**	100%	**58**	52	65	**32**	100%	**60**	55	69
BMI [kg/m²]	**50**	67,57%	**24,8**	21,7	29,4	**17**	70,83%	**24,8**	22,7	29,7	**23**	71,88%	**25,4**	21,6	29,4
TIPS_RRsys [mmHg]	**25**	33,78%	**116**	103	122	**10**	41,67%	**119**	106	130	**11**	34,38%	**107**	100	120
TIPS_RRdia [mmHg]	**25**	33,78%	**65**	57	70	**10**	41,67%	**68**	61	77	**11**	34,38%	**63**	55	69
TIPS_MAP [mmHg]	**26**	35,14%	**80,5**	74	91	**11**	45,83%	**88**	79	99	**11**	34,38%	**74**	72	85
TIPS_MELD	**70**	94,59%	**12**	10	19	**23**	95,83%	**13**	11	19	**30**	93,75%	**12**	11	17

Table 6: Appendix: all patients characteristics, overall and stratified by risk I

Abbreviations: BMI, body mass index; TIPS, transjugular intrahepatic portosystemic shunt; RRsys, systolic blood pressure; RRdia, diastolic blood pressure; MAP, mean arterial pressure; MELD, Model for Endstage Liver Disease;

		absolute frequency	relative frequency L %	absolute frequency	relative frequency L %	absolute frequency	relative frequency L %
SEX	female	27	36,5%	9	37,5%	11	34,4%
	male	47	63,5%	15	62,5%	21	65,6%
ETIOLOGY	alcohol related	55	75,3%	21	87,5%	25	78,1%
	not alcohol related	17	23,3%	3	12,5%	7	21,9%
	missing data	1	1,4%	0	0,0%	0	0,0%
TIPS_MainIndication	refraktärer Aszites	36	48,6%	13	54,2%	17	53,1%
	rezidivierende GI-Blutung (>2x)	14	18,9%	3	12,5%	9	28,1%
	aktive GI-Blutung	14	18,9%	5	20,8%	5	15,6%
	St. p. 1xBlutung, hohes Re-Blutungsrisiko	2	2,7%	1	4,2%	0	0,0%
	refraktärer Pleuraerguss re	4	5,4%	2	8,3%	1	3,1%
	HRS	1	1,4%	0	0,0%	0	0,0%
	partielle PVT	1	1,4%	0	0,0%	0	0,0%
	totale PVT	1	1,4%	0	0,0%	0	0,0%
	missing data	1	1,4%	0	0,0%	0	0,0%
Diab. Mell.	no	51	68,9%	19	79,2%	22	68,8%
	DM Type 1	10	13,5%	3	12,5%	3	9,4%
	DM Type 2	13	17,6%	2	8,3%	7	21,9%
TIPS_Child	A	5	6,76%	0	0,0%	4	50%
	B	46	16%	17	83%	19	38%
	C	8	81%	2	83%	4	50%
VHFA	missing data	15	27%	5	83%	5	63%
	yes	7	46%	2	8,3%	2	25%
	no	67	54%	22	91,6%	30	3,75%

Table 7: Appendix: all patients characteristics, overall and stratified by risk II

Abbreviations: TIPS, transjugular intrahepatic portosystemic shunt; HRS, hepato-renales syndrome; Diab. Mell., Diabetes Mellitus; VHFA,atrial fibrillation;